Gravitational waves from a string cusp in Einstein-aether theory

by

Marc Lalancette

B.Sc., Université de Montréal, 2003

A THESIS SUBMITTED IN PARTIAL FULFILMENT OF
THE REQUIREMENTS FOR THE DEGREE OF

Master of Science

in

The Faculty of Graduate Studies

(Physics)

The University Of British Columbia

(Vancouver)

April, 2008

Abstract

The motivation of this thesis is to look for a signature of Lorentz violation, hopefully observable, in the gravitational waves emitted by cosmic strings. Aspects of cosmic strings are reviewed, in particular how focused bursts of gravitational radiation are emitted when a cusp forms on the string. The same phenomenon is then studied in an effective field theory with Lorentz violation called Einstein-aether theory. This is a simple theory with a dynamic preferred frame, but it retains rotational and diffeomorphism invariance. The linearized version of the theory produces five wave modes. We study the usual transverse traceless modes which now have a wave speed that can be lower or greater than the speed of light. This altered speed produces distinctive features in the waves. They depend on two free parameters: roughly the wave speed and the acceleration of the string cusp. The profile of the wave is analysed in detail for different values of the parameters and explained by close comparison with the string motion.

Table of Contents

Appendices

List of Figures

Acknowledgements

I would like to thank my supervisor, Prof. Moshe Rozali, for helpful discussions and for his patience and understanding. I am also grateful to the department of physics for allowing me the time to complete my thesis. Finally, I want to thank my friends and family for their support and encouragement.

1. Introduction

Lorentz symmetry is a central component of our most successful physical theories. However, the possibility of departure from it at or near the Plank scale has received increased attention lately. One might question exact scale independence since it can never be tested (to arbitrarily high energies) even in principle. But more importantly, hints of Lorentz violation have appeared in our search for a quantum theory of gravity, the need to cut off high energy divergences of quantum field theory and perhaps even from experiment, in the possibly missing GZK cutoff of ultra high energy cosmic rays [1, and references].

The motivation of this thesis is to look for a signature of Lorentz violation, hopefully observable, in the gravitational waves emitted by cosmic strings. Cosmic strings are a particular case of a kind of field configuration known as topological defects. These highly energetic linear objects are predicted to form by a wide variety of elementary particle models at symmetry breaking phase transitions in the early Universe. For recent reviews see [2, 3, 4], see also [5, 6, 7]. Similar configurations exist in condensed matter systems, like vortex lines in liquid helium, flux tubes in type-II superconductors or disclination lines in liquid crystals.

The existence of a network of such strings has important cosmological implications. At first, they were considered a candidate to explain structure formation, providing density inhomogeneities, the seeds from which galaxies and clusters can grow. But studies of the cosmic microwave background have shown that cosmic strings (or other topological defects) could not explain most of the density perturbations. However, interest has been renewed by theoretical work on hybrid inflation and supersymmetric grand unified theories, by the discovery in string theory that fundamental strings or D-strings can in some scenarios play

the role of cosmic strings, and because we might soon be able to detect them.

It has been shown that cusps form generically when a string loop oscillates and that these cusps emit strong focused bursts of gravitational waves. It is this phenomenon that we will study in the presence of Lorentz violation. To do this, we will use an effective field theory that introduces a dynamic preferred frame by way of a unit timelike vector field dubbed the aether. The interaction of this aether field with the metric modifies the usual gravitational wave modes and the emitted spectrum by the string cusp.

This thesis is structured as follows. In chapter 1, we review some aspects of cosmic strings, including their nature, how they form at phase transitions and observable features of a cosmological network of such strings. We then touch on the superstring perspective before going into the dynamics of strings in more details. We briefly review how to calculate the gravitational waves generated by a source in chapter 2 and apply this to a string cusp in chapter 3. We obtain the spectrum and profile of the waves emitted by the cusp in the direction of its motion. In chapter 4, we consider Lorentz violation more closely and justify our choice of theory. Chapter 5 is a review of Einstein-aether theory, looking in details at the linearized wave modes. Finally we put the pieces together in chapter 6 where we compute the gravitational waves emitted by a cusp in Einstein-aether theory. We find distinctive features that may be detectable by planned gravitational wave detectors.

2. Cosmic strings

2.1 Topological defects

To understand the nature of the string, let us consider a simple model (Goldstone model) of a complex scalar field with a "mexican hat" potential (figure 2.1), described by the Lagrangian density

$$\begin{aligned} \mathcal{L} &= \partial_\mu \phi^* \partial^\mu \phi - V(\phi) \\ V(\phi) &= \frac{1}{2}\lambda \left(|\phi|^2 - \frac{1}{2}\eta^2 \right)^2 \end{aligned} \tag{2.1}$$

where λ and η are positive constants. This model has a global symmetry: it is invariant under the $U(1)$ group of phase transformations

$$\phi(x) \to e^{i\alpha}\phi(x) \tag{2.2}$$

with α constant. The ground state (or vacuum) has an expectation value on the circle $|\phi| = \eta$ at the bottom of the potential, with an arbitrary phase θ

$$\langle 0 \,|\phi|\, 0 \rangle = \eta e^{i\theta} \tag{2.3}$$

We see that the vacuum state is not invariant under the transformation, it changes the phase $\theta \to \theta + \alpha$. The symmetry is spontaneously broken.

Now let's assume that the field is in a vacuum state. Generically, the phase is free to vary continuously from point to point. If we find a closed curve in space where the phase

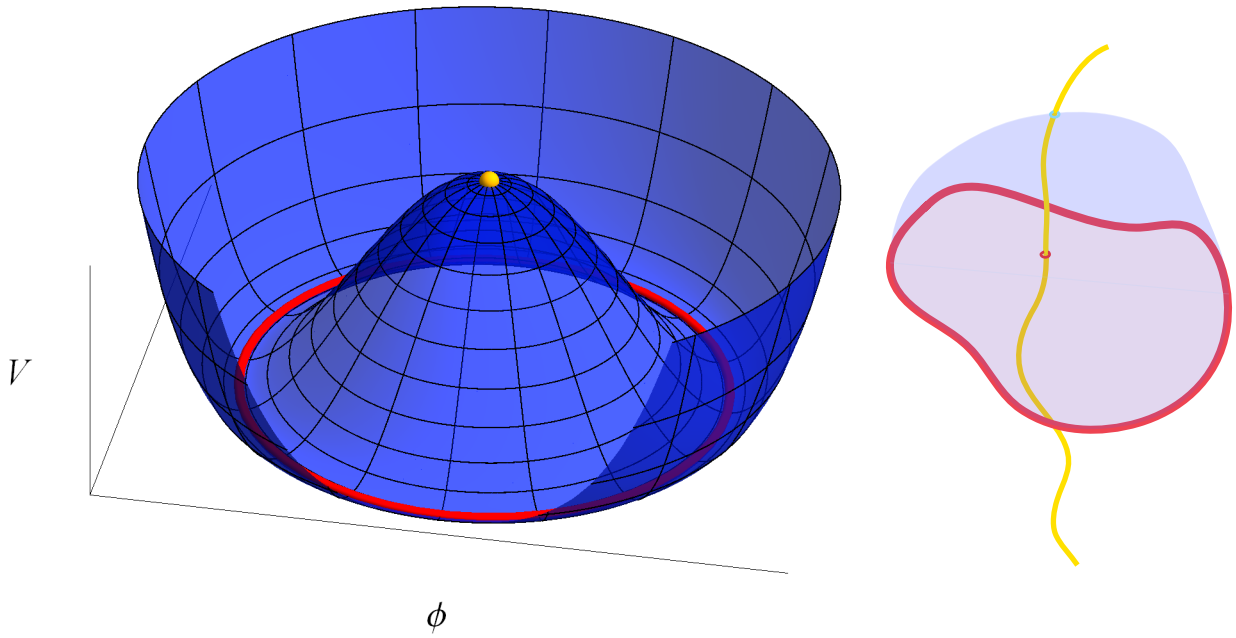

Figure 2.1: Potential for a complex scalar field in the Goldstone model. The minimum of the potential is degenerate as highlighted by the red circle (left). The yellow dot marks the local maximum at the origin. The drawing on the right shows a closed curve in space (red) where the field is at the minimum of the potential, winding once around the circle. Two surfaces bounded by this curve are drawn which are intersected by a curve (yellow) where $\phi = 0$.

winds once around the circle, then continuity demands that the field go through zero at a point (at least) on any surface bounded by that curve (see drawing in figure 2.1). Thus we find a linear region with non-zero energy density: a cosmic string. The gradient of the field also contributes to the energy and the string will have a certain width. When the broken symmetry is global as in this case, the solution is called a global string or vortex. Note that in this model, a static cylindrically symmetric string solution has an energy density that decays as ρ^{-2} at large radius ρ, so the energy per unit length of the string is infinite.

Strings can also form when the broken symmetry is local. A simple example is the Abelian Higgs model (or scalar electrodynamics) where we now introduce a vector field A_μ.

$$\begin{aligned} \mathcal{L} &= D_\mu \phi^* D^\mu \phi - \tfrac{1}{4} F_{\mu\nu} F^{\mu\nu} - V(\phi) \\ F_{\mu\nu} &= \partial_\mu A_\nu - \partial_\nu A_\mu \\ D_\mu &= \partial_\mu + ieA_\mu \end{aligned} \tag{2.4}$$

The symmetry transformation is now

$$\begin{aligned} \phi(x) &\rightarrow e^{i\alpha(x)} \phi(x) \\ A_\mu &\rightarrow A_\mu - \frac{1}{e} \partial_\mu \alpha(x) \end{aligned} \tag{2.5}$$

We again have a symmetry breaking vacuum state and string solutions. However, the energy density is now much more localized near the string center and the energy per unit length is finite. The string also caries magnetic flux and this will generate a repulsive force between strings since lines of flux repel each other. There is also an attractive force due to the scalar field because it is energically favorable to minimize the region of non-zero potential energy density. One of these forces will dominate depending on the masses of the vector and scalar modes about the vacuum.

In general, to see if string solutions or other defects exist for a particular model, we need to look at the topology of the vacuum manifold, the set of minima of the potential. Given

a gauge group G, we can find an unbroken subgroup H of transformations under which a vacuum solution is invariant (the isotropy group or little group). The vacuum manifold can then be identified as $\mathcal{M} = G/H$. A necessary condition for the existence of stable strings is that $\mathcal{M}$ be not simply connected, i.e. there are non-contractible loops in $\mathcal{M}$. Yet this condition is not sufficient in the sense that extra symmetry might extend the true vacuum manifold. For example, a semilocal model has both a global and a local symmetry and the vacuum manifold does not separate as the direct product of a local and a global part. The full vacuum manifold might be a sphere and the gauge orbit a circle on that sphere. A string configuration could then have zero potential energy density and have a tendency to spread out.

Similarly, if the vacuum manifold is not connected then there can be 2-dimensional domain walls separating regions in space where the field takes a vacuum value in different disconnected parts of $\mathcal{M}$. If $\mathcal{M}$ has the topology of a 2-sphere (it contains non-contractible surfaces), then there can be point-like monopoles. Finally, the topology of a 3-sphere can allow defects called textures. These are qualitatively different from other defects since the field is nowhere constrained to leave the minimum of the potential. Instead, they consist of non-trivial windings of the field when a uniform boundary condition is imposed at infinity. Effectively the boundary condition compactifies physical space. Note that stable defects cannot have free boundaries. For strings this means they will either form loops or extend to infinity, or in special scenarios they can end on monopoles. From this point we will only be interested in strings, mainly because in models where monopoles or domain walls are formed, they soon dominate the energy density of the universe and close it, unless they are formed before inflation, in which case they are too rare to be of interest.

2.2 Effective potential and phase transition

In the previous discussion, we treated the fields classically for simplicity, but for quantum fields we must take into account radiative corrections to the potential and look instead at the effective potential. Depending on the model, the corrections can be negligible or can drastically alter the potential. For example, the Abelian Higgs model with quadratic potential

$$V(\phi) = \mu_0^2 |\phi|^2 \tag{2.6}$$

appears to have unbroken symmetry, but its effective potential is

$$V_{\text{eff}}(\phi) = \mu_0^2 |\phi|^2 \left[1 + \nu^{-1} \frac{|\phi|^2}{\Lambda^2} \log \frac{|\phi|^2}{\Lambda^2}\right] \tag{2.7}$$

where Λ is the renormalization scale. When the dimensionless quantity $\nu = \frac{16\pi^2\mu_0^2}{3e^4\Lambda^2}$ becomes less than 0.37, then the absolute minimum will be away from $\phi = 0$ (figure 2.2 a).

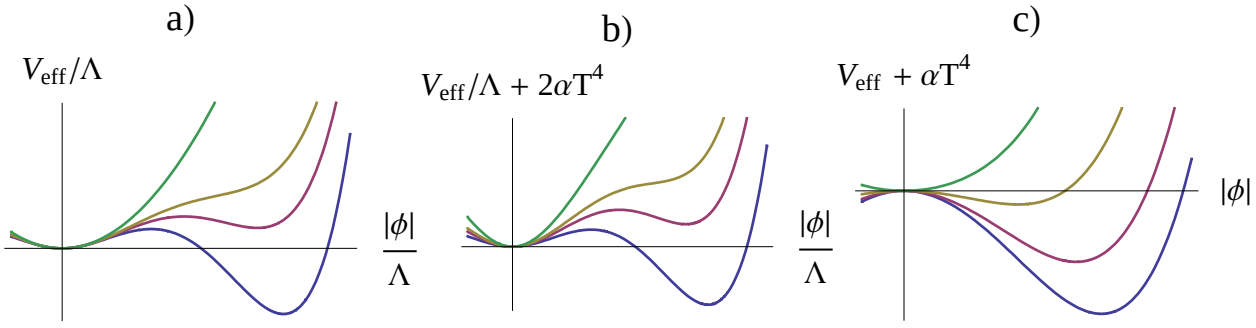

Figure 2.2: Profile of the effective potential of a complex scalar field in the Abelian-Higgs model (a, b) and Goldstone model (c). In a), we show the potential for decreasing (green to blue) values of the parameter ν. In b) and c) it is the temperature that decreases and we observe a phase transition of first and second order respectively.

To see how defects arise from phase transitions, we must consider the behavior of the fields at higher temperature (away from the ground state). We can do this by looking at the "finite-temperature effective potential", which is defined as the free energy density

$$V_{\text{eff}}(\phi, T) = (E - TS)/\mathcal{V} \tag{2.8}$$

(The name comes from the fact that the diagrammatic expansion is the same as for the effective potential, but with finite temperature Green's functions.) To first order in the coupling constants and for temperatures much higher than the mass thresholds, we have

$$V_{\text{eff}}(\phi, T) \approx V_{\text{eff}}(\phi) + \frac{1}{24}M^2T^2 - \frac{\pi^2}{90}NT^4 \tag{2.9}$$

where M^2 is a sum of particle masses and N is a sum of number of spin states.

For our Higgs model we find

$$V_{\text{eff}}(\phi, T) \approx \left(\mu_0^2 + \frac{1}{4}e^2T^2\right)|\phi|^2 + \frac{\mu_0^2|\phi|^4}{\nu\Lambda^2}\log\frac{|\phi|^2}{\Lambda^2} - \frac{2\pi^2}{45}T^4 \tag{2.10}$$

The profile of this potential for $\nu < 0.37$ at various temperatures is shown in figure 2.2 b. At high temperatures, the $T^2|\phi|^2$ term dominates and there is a single minimum at $\phi = 0$. As the temperature is lowered, a second minimum appears and below some critical temperature T_c it becomes lower than the minimum at $\phi = 0$. Such a discontinuous change in the value of $|\phi|$ at the minimum is a first-order phase transition. Note that the symmetric phase remains metastable all the way down to $T = 0$ for $\mu_0^2 > 0$ (although our expression is only valid for high temperatures).

As another example, the effective potential for the Goldstone model is

$$V_{\text{eff}}(\phi, T) \approx \frac{\lambda}{2}\left(\frac{1}{6}T^2 - \eta^2\right)|\phi|^2 + \frac{\lambda}{4}|\phi|^4 - \frac{\pi^2}{45}T^4 \tag{2.11}$$

In this case, as the temperature decreases below $T_c = \sqrt{6}\eta$, the symmetric state becomes unstable and the value of $|\phi|$ moves away from 0 continuously (figure 2.2 c). This is a second-order phase transition.

2.3 Formation and evolution of a string network

We can now see how strings can form in the early universe. Keeping with our simple models, as the universe expands after the Big Bang, the temperature decreases and the effective potential changes. Once the temperature reaches T_c, ϕ will start moving away from the symmetric state. However, the complex phase θ of ϕ will depend on random fluctuations. As the new state appears at different points in space, regions with different θ's will start expanding. When these regions meet, the field will adjust to remain continuous, but as we saw before, if the phase ends up winding on a closed curve in space, then the field will have to remain at 0 along a linear region, resulting in a cosmic string. Once the phase transition is over, we end up with a tangled string network.

Now in a realistic scenario, the final low-temperature symmetry group of the fields must be that of the Standard Model: $SU(3) \times U(1)$. We know that the weak and electromagnetic forces become united at a scale of about 100 GeV, and the gauge symmetry is enlarged from the electromagnetic $U(1)$ to an overall electroweak $SU(2) \times U(1)$. Similarly, the energy dependence of the strong and electroweak coupling strengths suggests that these interactions would also unite at an energy scale of 10^{15} or 10^{16} GeV into a grand unified theory. Such theories have been proposed based on various larger symmetry groups and symmetry breaking can occur in one or more steps from these groups down to $SU(3) \times SU(2) \times U(1)$. A detailed study of these theories shows that cosmic strings are generically formed [8].

The strength of the gravitational interaction of strings is characterized by the dimensionless parameter $G\mu$, where G is Newton's constant and μ is the energy per unit length, also equal to the string tension. For strings produced at a phase transition with temperature T_c, this is expected to be roughly T_c^2/M_p^2 where M_p is the Plank mass. At the grand unification scale, this corresponds to $G\mu \sim 10^{-6}$ or $\mu \sim 10^{21}\,\mathrm{kg/\,m}$ while at the electroweak scale,

$G\mu \sim 10^{-34}$ or $\mu \sim 10^{-7}\,\mathrm{kg/m}$. Note that stable strings are not formed in the electroweak model, but there are extensions of the Standard Model in which they are.

Once the universe is filled with a network of wiggly cosmic strings, they quickly develop relativistic speeds because of their tension. When two strings cross, they intercommute, i.e. the ends of the strings exchange partners. This happens with probability of order 1 for both global and local cosmic strings. This also leaves the strings with kinks at the crossing point. When a string intersects itself, a loop is cut off.

In an expanding universe, we could estimate that the total energy of infinite strings grows as the scaling factor a (the ratio of physical distance to distance in comoving coordinates) and so their energy density would scale as a^{-2}. This would lead to strings dominating over matter and radiation which scale as a^{-3} and a^{-4} respectively. Energy loss mechanisms however lead to a regime where strings provide a constant fraction of the energy density in an expanding universe. First, long strings will tend to straighten, reducing the total length, but this is offset by the formation of new kinks by string interaction. Second and most importantly, small loops (on scales shorter than the horizon) are not stretched and behave as matter. Finally, both kinks and loop oscillations will emit gravitational radiation and reduce the energy of the network, the loops eventually decaying completely. This scaling solution is an attractor, i.e. regardless of the initial distribution, the network will tend to this regime as long as there are some infinite strings. Simulations show that the ratio of string to matter energy density tends to $60G\mu$ (in the matter era), which is much too small to be a candidate for dark matter.

2.4 Observations

The most important observable effects of cosmic strings are believed to be gravitational. One place to look for their signature is in the cosmic microwave background (CMB) where statistical studies, pattern search [9, 10] and model likelihood analyses [11] have been performed. Originally, the possibility that strings might be an alternative to inflation for producing the primordial density perturbations generated a lot of interest. However, observations of the density perturbations and more recently the polarization of the CMB gave results in agreement with the inflation model, but difficult to explain by cosmic strings or other defects. On small scales, strings are expected to generate non-Gaussian perturbations. By determining how much the CMB temperature fluctuations deviate from Gaussian, we can find what fraction of the fluctuations might be due to strings. Many statistical studies agree that the contribution from cosmic strings is at most 10% and that $G\mu$ has an upper bound of order 10^{-6}.

On the other hand, spacetime around a string is conical, i.e. the total angle around the string is less than 2π, the deficit angle given by $8\pi G\mu$. Because of this, photons passing near a moving string will be red shifted if they pass in front and blue shifted behind. Hence strings would produce temperature step patterns that can be searched for directly in the CMB [12]. For a string with velocity β (and corresponding Lorentz factor γ), the height of the step would be $\frac{\Delta T}{T} \leq 8\pi G\mu\beta\gamma$. (The inequality represents the dependence on the orientations of the string and observer.)

One can also search for gravitational lensing effects due to strings. As of now, none have been found though there has been two candidates, one disproved [13], the other debatable [14]. Still, the search for lensed objects, in particular compact radio sources [15], could greatly improve constraints on cosmic string networks.

Other observable effects are due to the gravitational waves emitted by strings. First, they could be detected directly by planned experiments. It might appear at first that gravitational effects of strings with $G\mu \ll 10^{-7}$ would be too weak to be observed, but oscillating string loops will generically develop cusps which emit strong gravitational wave bursts (see section 3). Such bursts should be detectable by the Advanced LIGO and LISA detectors for $G\mu$ as low as 10^{-13}. The gravitational waves emitted since the formation of the network also add up to form a background with frequencies spanning several orders of magnitude. This background introduces noise in pulsar timing experiments. Current pulsar data yields $G\mu \leq 1.5 \times 10^{-8}$, a bound that could be lowered to 5×10^{-12} once the Parkes Pulsar Timing Array project is completed [16]. Such a bound would rule out many current models.

Finally, some cosmic strings can be superconducting and produce a variety of astrophysical effects even if they are light. They would interact strongly with magnetic fields and could produce gamma-ray bursts and high-energy cosmic rays [17].

2.5 String theory

The cosmic strings we have been considering so far are solitons of classical and quantum fields. We now address the possibility that superstrings might also form on large scales and act as cosmic strings [18]. For such strings to exist, there has to be a formation mechanism at the end of inflation, producing strings that are stable on cosmological time scale and with tensions not already ruled out by observations. Some models satisfy all these conditions and might have some distinctive characteristics. In fact, cosmic strings could provide the best observational window into string theory.

In the context of perturbative string theory, cosmic strings are ruled out since funda-

mental strings have tensions close to the Planck scale. However, the geometry of compact dimensions was found to have more general possibilities than previously thought, and tensions can be much lower, all the way down to the weak scale. For example, if the gauge fields are confined on a brane while gravity propagates in the bulk with extra dimensions of size R, then the tension is suppressed by some power of $\frac{R}{L_p}$ where L_p the Planck length. Even without large extra dimensions, the effective tension can be reduced by bulk gravitational potentials. Also, the role of cosmic strings can be played by D-strings or higher dimensional D-branes with $D-1$ compact dimensions, which look like strings on a macroscopic scale.

In models of brane inflation, colliding branes generate a network of cosmic strings in many cases. In fact, in what seems to be the most natural model (KKLMMT) strings are produced but not the problematic monopoles or domain walls. In these models, the value of $G\mu$ can be deduced from the CMB fluctuations. It is expected to be in the range $[10^{-11}, 10^{-6}]$.

Some cosmic strings can be subject to instabilities, even in field theory [19]. There are general arguments in string theory that there are no exact global symmetries. Also the no-hair theorem implies that black holes can destroy global charges and they are not exactly conserved. If the symmetry is not exact, the vacuum is not exactly degenerate. This leads to the formation of domain walls bounded by the strings and their tension forces the network to collapse. For gauge symmetries, it is generally expected in unified theories that there are sources for every flux. Then strings can break into short segments by creation of monopole-antimonopole pairs. In string theory, coupling of strings to form fields can also lead to breakage. However, there are still stable candidates. In particular, in inflation models, features such as large dimensions or warping can stabilize strings.

One of the main distinctive features of cosmic superstrings is that the probability of intercommuting can be much less than 1. For fundamental strings, it is a quantum process

with a probability of order g_s^2. Also in many cases, strings can move in the compact dimensions and so can miss each other. However in realistic compactifications they will be confined by a potential in these dimensions. For different models, the reconnection probability for fundamental strings ranges from 10^{-3} to 1 while for D-strings it goes from 10^{-1} to 1. For collisions involving one of each, the probability can vary from 0 to 1. With a probability much smaller than 1, the number of strings should be larger. This feature may help distinguish a string theory network from a field theory one.

2.6 String dynamics and cusps

We now wish to find a simplified general model to study the motion of a string at low temperature and small string curvature. At low energies, we do not expect significant excitation of the massive modes, like oscillations of the string thickness. If we integrate out these modes, we find a low energy effective action proportional to the area of the worldsheet, the two-dimensional surface swept out by the motion of the string (neglecting its width). We can also justify this action by general arguments. First, if the radius of curvature R is much larger than the string thickness δ, we can consider the string as a one-dimensional object. For gauge strings, where there is no long range interaction between string segments, we should be able to write a local action of the form

$$S = \int d^2\sigma \, \sqrt{-\gamma}\mathcal{L} \tag{2.12}$$

where σ^0, σ^1 are worldsheet coordinates and γ is the determinant of the induced metric on the worldsheet $\gamma_{ab} = X^\mu{}_{,a} X^\nu{}_{,b} g_{\mu\nu}$, $X^\mu(\sigma^0, \sigma^1)$ being the spacetime coordinates of the string. The Lagrangian density must be invariant under spacetime and worldsheet coordinate transformations so it can only depend on the string tension and geometric quantities such as curvature. But typically, the string thickness is $\gtrsim \mu^{-1/2}$ while curvature is of order

R^{-2}. Thus we can neglect curvature terms and we are left with the Nambu-Goto action

$$S = -\mu \int d^2\sigma \sqrt{-\gamma} \tag{2.13}$$

We next find the equations of motion in flat spacetime $\eta_{\mu\nu} = \text{diag}\,(-,+,+,+)$. Defining

$$\begin{aligned} \dot{X}^\mu &\equiv \partial_{\sigma^0} X^\mu \\ X'^\mu &\equiv \partial_{\sigma^1} X^\mu \end{aligned} \tag{2.14}$$

we choose the following gauge conditions on the worldsheet:

$$\begin{aligned} X^0 &= \sigma^0 \\ \dot{X} \cdot X' &= 0 \\ \dot{X}^2 + X'^2 &= 0 \end{aligned} \tag{2.15}$$

The first condition is simply to take σ^0 as being our time coordinate. The second condition ensures that the motion of a point on the string with fixed σ^1 will be perpendicular to the shape of the string at any given time. Then $\dot{\mathbf{X}}$ is the transverse velocity of the string. The third condition then implies that the energy is distributed uniformly in terms of the σ^1 parameterization. To see this, use the first condition to write the others as

$$\begin{aligned} \dot{\mathbf{X}} \cdot \mathbf{X}' &= 0 \\ \dot{\mathbf{X}}^2 + \mathbf{X}'^2 &= 1 \end{aligned} \tag{2.16}$$

and then, looking back at the Lagrangian, we find the Hamiltonian density:

$$\begin{aligned} \mathcal{H} &= \frac{\partial \mathcal{L}}{\partial \dot{X}^i} \dot{X}^i - \mathcal{L} \\ &= \mu \frac{\mathbf{X}'^2}{\sqrt{\left(\dot{\mathbf{X}} \cdot \mathbf{X}'\right)^2 + \left(1 - \dot{\mathbf{X}}^2\right) \mathbf{X}'^2}} \\ &\to \mu \end{aligned} \tag{2.17}$$

So we see indeed that in this gauge, the energy density is simply the constant μ, and the total energy, $E = \mu \int d\sigma^1$. In terms of proper length then the energy of a segment $ds = |\mathbf{X}'|\, d\sigma^1$ is just the relativistic expression for the energy of a particle of mass $\mu\, ds$: $\frac{\mu\, ds}{\sqrt{1-\dot{\mathbf{X}}^2}}$. We also define the "invariant length" of the string to be $l \equiv \frac{E}{\mu}$, and we can then choose $\sigma^1 \in [0, l]$. The last two conditions imply that the induced metric is conformally flat:

$$\gamma_{ab} = \sqrt{-\gamma}\eta_{ab}, \quad \gamma^{ab} = \frac{1}{\sqrt{-\gamma}}\eta^{ab} \tag{2.18}$$

and so this choice is called a "conformal gauge".

Varying the action with respect to X_μ and then imposing our gauge gives

$$\delta S = -\mu \int d^2\sigma \, \left[\partial_{\sigma^0}\left(\delta X_\mu \dot{X}^\mu\right) - \partial_{\sigma^1}\left(\delta X_\mu X'^\mu\right) + \delta X_\mu \left(X''^\mu - \ddot{X}^\mu\right)\right] \tag{2.19}$$

The first term vanishes for variations with fixed initial and final states. The second term gives the boundary conditions for open strings

$$\int d\sigma^0 \, \left[\delta X_\mu X'^\mu\right]_0^l = 0 \tag{2.20}$$

implying either fixed ends ($\delta X = 0$) or free ends that move at the speed of light ($X'^2 = 1 - \dot{\mathbf{X}}^2 = 0$). The last term in the variation gives us the equation of motion, a wave equation:

$$\ddot{\mathbf{X}} - \mathbf{X}'' = 0 \tag{2.21}$$

Our work will be simplified with the use of null worldsheet coordinates $\sigma_\pm = \sigma^0 \pm \sigma^1$. The general solution is then expressed as the sum of two functions (the so-called left and right movers)

$$\mathbf{X}\left(\sigma^0, \sigma^1\right) = \frac{1}{2}\left[\mathbf{X}_+\left(\sigma_+\right) + \mathbf{X}_-\left(\sigma_-\right)\right] \tag{2.22}$$

and our gauge constraints (2.15) become

$$\dot{\mathbf{X}}_+^2 = \dot{\mathbf{X}}_-^2 = 1 \tag{2.23}$$

Differentiating these yields the useful relations

$$\begin{aligned} \dot{X}_\pm \cdot \ddot{X}_\pm &= 0 \\ \dot{X}_\pm \cdot \dddot{X}_\pm + \ddot{X}_\pm^2 &= 0 \end{aligned} \tag{2.24}$$

It is easy to see that the motion of a closed string will also be periodic in time (in the center-of-mass frame), but with period $\frac{l}{2}$ since $\mathbf{X}\left(\sigma^0 + \frac{l}{2}, \sigma^1 + \frac{l}{2}\right) = \mathbf{X}\left(\sigma^0, \sigma^1\right)$.

Periodicity in both space and time requires

$$\int_0^l d\sigma_+ \, \dot{\mathbf{X}}_+ = \int_0^l d\sigma_- \, \dot{\mathbf{X}}_- = 0 \tag{2.25}$$

With the unit constraint (2.23), this means that $\dot{\mathbf{X}}_\pm$ trace out a pair of curves on the unit sphere, each with its centroid at the center of the sphere. So in particular, a curve cannot lie in one hemisphere and they will be expected to cross in generic cases. When this happens, we find that at that point (which we'll call X_0)[1], the speed on the string will be the speed of light:

$$\dot{\mathbf{X}}_0^2 = \frac{1}{4}\left[\dot{\mathbf{X}}_{+0} + \dot{\mathbf{X}}_{-0}\right]^2 = \dot{\mathbf{X}}_{\pm 0}^2 = 1 \tag{2.26}$$

If the string has kinks, there are discontinuities in $\dot{\mathbf{X}}_\pm$, meaning gaps in the curves on the sphere and it is much easier for them not to intersect and avoid these luminal points. To visualize the shape of the string around the luminal point, we use a Taylor expansion in $\sigma_\pm$, with $\mathbf{X}_0$ at the origin.

$$\begin{aligned} X_\pm^\mu &\simeq \dot{X}_{\pm 0}^\mu \sigma_\pm + \frac{1}{2}\ddot{X}_{\pm 0}^\mu \sigma_\pm^2 + \frac{1}{6}\dddot{X}_{\pm 0}^\mu \sigma_\pm^3 \\ \mathbf{X}\left(0, \sigma\right) &\simeq \frac{1}{2}\ddot{\mathbf{X}}_0 \sigma^2 + \frac{1}{12}\left(\dddot{\mathbf{X}}_{+0} - \dddot{\mathbf{X}}_{-0}\right)\sigma^3 \end{aligned} \tag{2.27}$$

We see that the string will develop a cusp at that moment and it is the tip of the cusp that is luminal (figure 2.3). The relation (2.24) shows that the tip moves transversely as expected:

$$\dot{\mathbf{X}}_0 \cdot \ddot{\mathbf{X}}_0 = 0 \tag{2.28}$$

[1]The notation here shouldn't cause any confusion since in our gauge the component X^0 has been fixed and we don't use it henceforth.

We now return to the action and vary it with respect to the spacetime metric. Recalling that the variation of a determinant is

$$\delta \det A = \det A \operatorname{tr}\left(A^{-1}\delta A\right) \tag{2.29}$$

we find

$$\begin{aligned} \delta S &= -\mu \int d^2\sigma \, \frac{1}{2} \frac{\gamma \gamma^{ab} \delta \gamma_{ab}}{\sqrt{-\gamma}} \\ &= \frac{\mu}{2} \int d^2\sigma \, \sqrt{-\gamma} \gamma^{ab} X^{\mu}{}_{,a} X^{\nu}{}_{,b} \delta g_{\mu\nu} \\ &= \frac{\mu}{2} \int d^4x \int d^2\sigma \, \sqrt{-\gamma} \gamma^{ab} x^{\mu}{}_{,a} x^{\nu}{}_{,b} \delta^{(4)}\left(X - x\right) \delta g_{\mu\nu} \end{aligned} \tag{2.30}$$

So the energy momentum tensor is

$$\begin{aligned} T^{\mu\nu}\left(x\right) &= -\frac{2}{\sqrt{-g}} \frac{\delta \mathcal{L}}{\delta g_{\mu\nu}} \\ &= -\frac{\mu}{\sqrt{-g}} \int d^2\sigma \, \sqrt{-\gamma} \gamma^{ab} x^{\mu}{}_{,a} x^{\nu}{}_{,b} \delta^{(4)}\left(X - x\right) \end{aligned} \tag{2.31}$$

In flat spacetime and in our gauge, this becomes

$$T^{\mu\nu}\left(x\right) = \mu \int d^2\sigma \, \left(\dot{x}^{\mu}\dot{x}^{\nu} - x'^{\mu}x'^{\nu}\right) \delta^{(4)}\left(X - x\right) \tag{2.32}$$

Later, we will use the Fourier transform

$$\begin{aligned} T^{\mu\nu}\left(x\right) &= \frac{1}{\left(2\pi\right)^4} \int_{-\infty}^{\infty} d\omega \int d^3\boldsymbol{k} \, e^{ik\cdot x} T^{\mu\nu}\left(k\right) \\ T^{\mu\nu}\left(k\right) &= \int_{-\infty}^{\infty} dt \int d^3\boldsymbol{x} \, e^{-ik\cdot x} T^{\mu\nu}\left(x\right) \end{aligned} \tag{2.33}$$

In terms of our null coordinate solution, we obtain

$$\begin{aligned} T^{\mu\nu}\left(k\right) &= \mu \int d^2\sigma \, \left(\dot{X}^{\mu}\dot{X}^{\nu} - X'^{\mu}X'^{\nu}\right) e^{-ik\cdot X} \\ &\equiv \frac{\mu}{2} I_{+}^{(\mu} I_{-}^{\nu)} \\ I_{\pm}^{\mu} &= \int_{-\frac{l}{2}}^{\frac{l}{2}} d\sigma_{\pm} \, \dot{X}_{\pm}^{\mu} \, e^{-\frac{i}{2}k\cdot X_{\pm}} \end{aligned} \tag{2.34}$$

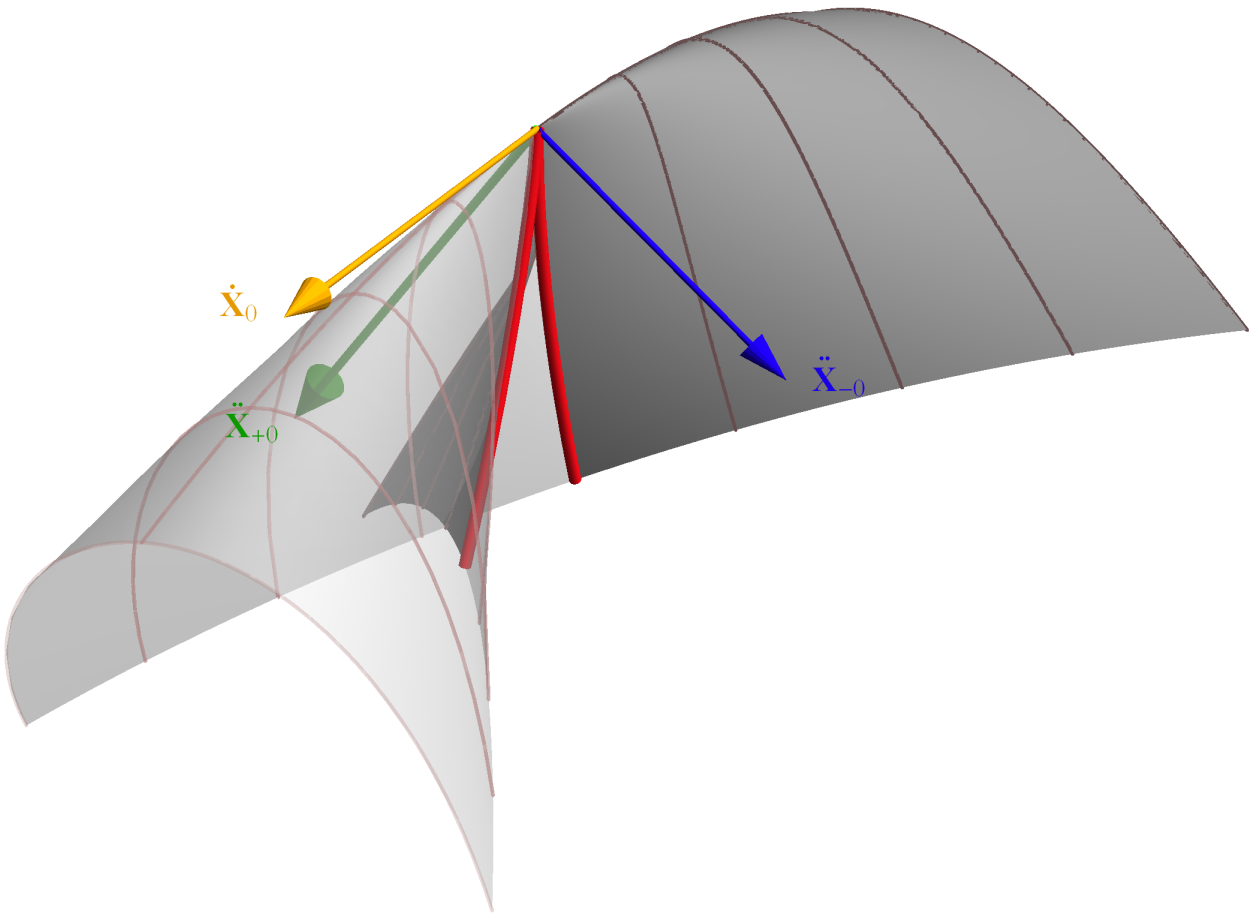

Figure 2.3: String worldsheet around a cusp. The lines on the worldsheet show the string at given times, in particular at the moment of the cusp formation (in red). Also shown are the speed vector (in yellow) and in a plane perpendicular to it, the acceleration vectors for the + and - components of the string solution (in green and blue).

3. Gravitational waves

We now briefly review how the linearized Einstein equations lead to gravitational waves and we find an expression for the metric perturbation far from a localized source. First, we assume that the metric is nearly flat and write it as

$$\begin{aligned} g_{\mu\nu} &= \eta_{\mu\nu} + h_{\mu\nu} \\ |h_{\mu\nu}| &\ll 1 \end{aligned} \tag{3.1}$$

Indices are raised and lowered with $\eta_{\mu\nu}$ so to first order in h, the inverse metric is $g^{\mu\nu} = \eta^{\mu\nu} - h^{\mu\nu}$. We will also use the trace-reversed metric perturbation:

$$\bar{h}_{\mu\nu} = h_{\mu\nu} - \frac{1}{2}\eta_{\mu\nu}h^{\alpha}{}_{\alpha} \tag{3.2}$$

The allowed transformations that preserve the smallness of the perturbation are global Lorentz transformations

$$h_{\mu\nu} \to \Lambda^{\alpha}{}_{\mu}\Lambda^{\beta}{}_{\nu}h_{\alpha\beta} \tag{3.3}$$

and small coordinate transformations

$$\begin{aligned} x^{\mu} &\to y^{\mu} = x^{\mu} + \varepsilon^{\mu} \\ J^{\mu}{}_{\nu} &\equiv \frac{\partial y^{\mu}}{\partial x^{\nu}} = \delta^{\mu}{}_{\nu} + \varepsilon^{\mu}{}_{,\nu} \end{aligned} \tag{3.4}$$

Under an infinitesimal coordinate transformation, tensors pick up a Lie derivative [see appendix A], i.e. with indices suppressed:

$$T'(x) = T(x) - \mathcal{L}_{\varepsilon}T(x) \tag{3.5}$$

where on the left, x is taken as a value of the new coordinates. On the metric this gives

$$\begin{aligned} g'_{\mu\nu} &\approx g_{\mu\nu} - \varepsilon^{\lambda}{}_{,\mu} g_{\lambda\nu} - \varepsilon^{\lambda}{}_{,\nu} g_{\mu\lambda} - \varepsilon^{\lambda} g_{\mu\nu,\lambda} \\ h'_{\mu\nu} &\approx h_{\mu\nu} - \varepsilon^{\lambda}{}_{,\mu}\eta_{\lambda\nu} - \varepsilon^{\lambda}{}_{,\nu}\eta_{\mu\lambda} - \varepsilon^{\lambda} h_{\mu\nu,\lambda} \\ &= h_{\mu\nu} - 2\varepsilon_{(\mu,\nu)} - \varepsilon^{\lambda} h_{\mu\nu,\lambda} \\ \bar{h}'_{\mu\nu} &= \bar{h}_{\mu\nu} - 2\varepsilon_{(\mu,\nu)} + \eta_{\mu\nu}\varepsilon^{\lambda}{}_{,\lambda} - \varepsilon^{\lambda}\bar{h}_{\mu\nu,\lambda} \end{aligned} \tag{3.6}$$

We see that in order for h' to remain small, we need $\left|\varepsilon^{\mu}{}_{,\nu}\right| \ll 1$. The last term is usually thrown away, taking only the terms first order in both h and ε. This presupposes that both ε and the derivatives of h are also $\ll 1$. However the requirement on ε is only that the product $\varepsilon^{\lambda} h_{\mu\nu,\lambda}$ be small and so in general, the term should be kept. Of course, if we choose an appropriately small ε (depending on how small the derivatives are) then we can neglect the term.

To first order in the perturbation h, the Ricci and Einstein tensors are

$$\begin{aligned} R^{(1)}_{\mu\nu} &= -2\eta^{\kappa\lambda} h_{\llcorner\kappa\ulcorner\lambda,\mu\lrcorner\nu\urcorner} \equiv -\frac{1}{2}\eta^{\kappa\lambda}\left(h_{\kappa\lambda,\mu\nu} - h_{\kappa\nu,\mu\lambda} + h_{\mu\nu,\kappa\lambda} - h_{\mu\lambda,\kappa\nu}\right) \\ G^{(1)}_{\mu\nu} &= -2\eta^{\kappa\lambda} h_{\llcorner\kappa\ulcorner\lambda,\mu\lrcorner\nu\urcorner} + \eta_{\mu\nu}\eta^{\alpha\beta}\eta^{\kappa\lambda} h_{\llcorner\kappa\lambda,\alpha\lrcorner\beta} \end{aligned} \tag{3.7}$$

To solve the linearized field equation $G^{(1)}_{\mu\nu} = 8\pi G T_{\mu\nu}$, we first choose a gauge. We apply the harmonic gauge condition:

$$\begin{aligned} \Box x^{\alpha} &\equiv g^{\mu\nu} x^{\alpha}{}_{;\mu\nu} = 0 \\ &\Rightarrow g^{\mu\nu}\Gamma^{\alpha}_{\mu\nu} = 0 \\ &\Rightarrow \left(\sqrt{-g}\, g^{\mu\nu}\right)_{,\mu} = 0 \end{aligned} \tag{3.8}$$

To first order in h, this corresponds to the condition $\bar{h}^{\mu\nu}{}_{,\nu} = 0$. This partial gauge choice still allows global Lorentz transformations and coordinate transformations (3.4) with $\Box\varepsilon^{\mu} = 0$. This gauge also simplifies the Einstein tensor, and the field equation is now

$$G^{(1)}_{\mu\nu} = -\frac{1}{2}\eta^{\kappa\lambda}\bar{h}_{\mu\nu,\kappa\lambda} = 8\pi G\, T_{\mu\nu} \tag{3.9}$$

In vacuum, the general solution is a sum of plane waves of the form

$$\begin{aligned} \bar{h}_{\mu\nu} &= \mathrm{Re}\left\{A_{\mu\nu}e^{ik\cdot x}\right\} \\ k_\mu k^\mu &= 0 \end{aligned} \tag{3.10}$$

Our harmonic gauge choice further imposes $A_{\mu\nu}k^\mu = 0$. Next we fix (most of) the remaining freedom by imposing the transverse traceless (TT) gauge conditions [20, chapter 35.4]:

$$A_{\mu 0} = A_\mu^{\ \mu} = 0 \tag{3.11}$$

Equivalently, we can write the TT gauge as 8 conditions (including the harmonic gauge conditions) on h:

$$h_{\mu 0} = h_{ii} = h_{ij,j} = 0 \tag{3.12}$$

This leaves 2 degrees of freedom (out of the 10 components of h). We are still allowed spatial rotations, so we can fix $k^\mu = (\omega, 0, 0, \omega)$, leaving only rotations in the xy plane as remaining freedom. The two linear polarizations are called $+$ and $\times$ and are defined as

$$\epsilon_\oplus^{\mu\nu} \equiv \begin{bmatrix} 0 & 0 & 0 & 0 \\ 0 & 1 & 0 & 0 \\ 0 & 0 & -1 & 0 \\ 0 & 0 & 0 & 0 \end{bmatrix}, \quad \epsilon_\otimes^{\mu\nu} \equiv \begin{bmatrix} 0 & 0 & 0 & 0 \\ 0 & 0 & 1 & 0 \\ 0 & 1 & 0 & 0 \\ 0 & 0 & 0 & 0 \end{bmatrix} \tag{3.13}$$

Any pure wave in linearized theory can be reduced to this gauge.

We also want to solve (3.9) far from a localized source, more precisely in the "wave zone" where $r \equiv |\boldsymbol{x}|$ is much larger than the source but still much smaller than the Hubble radius. We solve this by using a Green's function, i.e. we find a solution $H(x)$ to

$$-\frac{1}{2}\eta^{\kappa\lambda}H_{,\kappa\lambda}(x) = \delta^{(4)}(x) \tag{3.14}$$

and the general solution to is then

$$\bar{h}_{\mu\nu}(x) = 8\pi G \int d^4y\, H(x-y)\, T_{\mu\nu}(y) \tag{3.15}$$

To solve (3.14), we go to Fourier space

$$\begin{aligned} -\frac{1}{2}\eta^{\kappa\lambda}\int\frac{d^4k}{(2\pi)^4}\partial_\kappa\partial_\lambda e^{ik\cdot x}H(k) &= \int\frac{d^4k}{(2\pi)^4}e^{ik\cdot x} \\ H(k) &= \frac{2}{k^2} \end{aligned} \tag{3.16}$$

and so

$$\begin{aligned} H(x) &= 2\int\frac{d^4k}{(2\pi)^4}\frac{e^{ik\cdot x}}{k^2} \\ &= 2\int\frac{d^3k}{(2\pi)^4}e^{i\boldsymbol{k}\cdot\boldsymbol{x}}\int_{-\infty}^{\infty}d\omega\,\frac{e^{-i\omega t}}{\boldsymbol{k}^2-\omega^2} \end{aligned} \tag{3.17}$$

There are 2 poles on the real axis of this last integral. We can evaluate it by first closing a contour with a semicircle of infinite radius in the upper or lower half plane for $t<0$ or >0 respectively ($\omega=\Omega e^{\pm i\theta}$), on which the integral vanishes:

$$\begin{aligned} \lim_{\Omega\to\infty}\left|\int_0^\pi\frac{e^{-i\Omega(\cos\theta\pm i\sin\theta)t}}{\boldsymbol{k}^2-\Omega^2e^{\pm2i\theta}}\Omega ie^{\pm i\theta}\,d\theta\right| &\leq \lim_{\Omega\to\infty}\int_0^\pi\frac{\Omega e^{-\Omega|t|\sin\theta}}{\left|\boldsymbol{k}^2-\Omega^2e^{\pm2i\theta}\right|}\,d\theta \\ &\leq \lim_{\Omega\to\infty}\frac{\Omega}{\left(\Omega^2+\boldsymbol{k}^2\right)}\int_0^\pi d\theta \\ &= 0 \end{aligned} \tag{3.18}$$

We want the retarded Green's function, i.e. $H(t<0)=0$, so we add an infinitesimal imaginary part to ω

$$\int_{-\infty}^{\infty}d\omega\,\frac{e^{-i\omega t}}{-\left(\omega-|\boldsymbol{k}|+i\epsilon\right)\left(\omega+|\boldsymbol{k}|+i\epsilon\right)} \tag{3.19}$$

and use Cauchy's integral formula:

$$\oint dz\,\frac{f(z)}{z-z_0}=2\pi i f(z_0) \tag{3.20}$$

For $t>0$, there is an extra minus sign from moving in the clockwise direction along the contour and we pick both poles. The residues are

$$\begin{aligned} \omega &= |\boldsymbol{k}|-i\epsilon:\frac{-e^{-i|\boldsymbol{k}|t-\epsilon t}}{2|\boldsymbol{k}|}\to\frac{-e^{-i|\boldsymbol{k}|t}}{2|\boldsymbol{k}|} \\ \omega &= -|\boldsymbol{k}|-i\epsilon:\frac{-e^{i|\boldsymbol{k}|t-\epsilon t}}{-2|\boldsymbol{k}|}\to\frac{e^{i|\boldsymbol{k}|t}}{2|\boldsymbol{k}|} \end{aligned} \tag{3.21}$$

So our integral is now

$$\begin{aligned} H(x) &= -\frac{i}{2}2\int \frac{d^3k}{(2\pi)^3}\frac{e^{i\boldsymbol{k}\cdot\boldsymbol{x}}}{|\boldsymbol{k}|}\left(e^{i|\boldsymbol{k}|t}-e^{-i|\boldsymbol{k}|t}\right)\theta(t) \\ &= i\theta(t)\int_0^\infty \frac{d|\boldsymbol{k}|\ \boldsymbol{k}^2}{(2\pi)^2}\frac{e^{i|\boldsymbol{k}|t}-e^{-i|\boldsymbol{k}|t}}{|\boldsymbol{k}|}\int_1^{-1} d(\cos\theta)\ e^{i|\boldsymbol{k}||\boldsymbol{x}|\cos\theta} \\ &= i\theta(t)\int_0^\infty \frac{d|\boldsymbol{k}|}{(2\pi)^2}|\boldsymbol{k}|\left(e^{i|\boldsymbol{k}|t}-e^{-i|\boldsymbol{k}|t}\right)\frac{e^{-i|\boldsymbol{k}||\boldsymbol{x}|}-e^{i|\boldsymbol{k}||\boldsymbol{x}|}}{i|\boldsymbol{k}||\boldsymbol{x}|} \\ &= \frac{\theta(t)}{2\pi|\boldsymbol{x}|}\int_{-\infty}^\infty \frac{d|\boldsymbol{k}|}{2\pi}\left(e^{i|\boldsymbol{k}|(t-|\boldsymbol{x}|)}-e^{-i|\boldsymbol{k}|(t+|\boldsymbol{x}|)}\right) \\ &= \frac{\theta(t)}{2\pi|\boldsymbol{x}|}\delta(t-|\boldsymbol{x}|) \end{aligned} \tag{3.22}$$

In the last step, the second δ-function vanishes because of the step function. So (3.15) becomes

$$\begin{aligned} \bar{h}_{\mu\nu}(x) &= 4G\int d^4y\frac{\theta(x_0-y_0)}{|\boldsymbol{x}-\boldsymbol{y}|}\delta(x_0-y_0-|\boldsymbol{x}-\boldsymbol{y}|)\,T_{\mu\nu}(y) \\ &= 4G\int d^3y\frac{T_{\mu\nu}(x_0-|\boldsymbol{x}-\boldsymbol{y}|,\boldsymbol{y})}{|\boldsymbol{x}-\boldsymbol{y}|} \\ &= 4G\int\frac{d\omega}{2\pi}\int d^3y\,e^{-i\omega(x_0-|\boldsymbol{x}-\boldsymbol{y}|)}\frac{T_{\mu\nu}(\omega,\boldsymbol{y})}{|\boldsymbol{x}-\boldsymbol{y}|} \end{aligned} \tag{3.23}$$

In the wave zone, $r\equiv|\boldsymbol{x}|\gg|\boldsymbol{y}|$ so we can approximate

$$\begin{aligned} |\boldsymbol{y}-\boldsymbol{x}| &= \sqrt{r^2-2\boldsymbol{x}\cdot\boldsymbol{y}+\boldsymbol{y}^2} \\ &\approx r\left(1-\frac{\boldsymbol{x}\cdot\boldsymbol{y}}{r^2}+\frac{\boldsymbol{y}^2}{2r^2}\right) \end{aligned} \tag{3.24}$$

$$\bar{h}_{\mu\nu}(x)\approx 4G\int\frac{d\omega}{2\pi}\int d^3y\,e^{-i\omega\left(x_0-r+\frac{\boldsymbol{x}}{r}\cdot\boldsymbol{y}\right)}\frac{T_{\mu\nu}(\omega,\boldsymbol{y})}{r} \tag{3.25}$$

For the approximation in the phase factor to be valid, we require $\frac{\boldsymbol{y}^2}{2r^2}\ll\frac{1}{|\omega|}$, so we need a large r to investigate high frequencies. Define the retarded time $t_R=t-r$ and the wave-vector

in the direction of the observer $k_{\boldsymbol{x}} = \omega\left(1, \frac{\boldsymbol{x}}{r}\right)$ and we get

$$\begin{aligned} \bar{h}_{\mu\nu}\left(t_R, \boldsymbol{x}\right) &= \frac{2G}{\pi}\int d\omega\, \frac{e^{-i\omega t_R}}{r}\int d^3\boldsymbol{y}\, e^{-i\boldsymbol{k_x}\cdot\boldsymbol{y}} T_{\mu\nu}\left(\omega, \boldsymbol{y}\right) \qquad (3.26) \\ &= \frac{2G}{\pi r}\int d\omega\, e^{-i\omega t_R} T_{\mu\nu}\left(k_{\boldsymbol{x}}\right) \\ \bar{h}^{\mu\nu}\left(\omega, \boldsymbol{x}\right) &= \frac{4G}{r} T_{\mu\nu}\left(k_{\boldsymbol{x}}\right) \qquad (3.27) \end{aligned}$$

4. Waves from a string cusp

Following [21], we now find the gravitational wave spectrum emitted by a string cusp in the direction of its motion, $k = \omega \dot{X}_0$, far from the string. Inserting (2.34) into (3.27) we get

$$\bar{h}^{\mu\nu}(\omega, \boldsymbol{x}) = \frac{2G\mu}{r} I_+^{(\mu} I_-^{\nu)} \tag{4.1}$$

Using the expansion (2.27) about the cusp, the leading terms in our integrals are now

$$\begin{aligned} I_\pm^\mu &= \int_{-\frac{l}{2}}^{\frac{l}{2}} d\sigma_\pm \, \dot{X}_\pm^\mu \, e^{-\frac{i}{2} k \cdot X_\pm} \\ &\approx \int_{-\frac{l}{2}}^{\frac{l}{2}} d\sigma_\pm \left(\dot{X}_{\pm 0}^\mu + \ddot{X}_{\pm 0}^\mu \sigma_\pm \right) e^{-\frac{i}{2} \omega \dot{X}_0 \cdot X_\pm} \end{aligned} \tag{4.2}$$

To simplify the phase, we use $\dot{X}_0 = \dot{X}_{\pm 0}$ (2.26), and the gauge constraints (2.23) and (2.24). This gives

$$\begin{aligned} \dot{X}_0 \cdot X_\pm &= \dot{X}_{\pm 0} \cdot \left(\dot{X}_{\pm 0} \sigma_\pm + \frac{1}{2} \ddot{X}_{\pm 0} \sigma_\pm^2 + \frac{1}{6} \dddot{X}_{\pm 0} \sigma_\pm^3 \right) \\ &= -\frac{1}{6} \ddot{X}_\pm^2 \sigma_\pm^3 \end{aligned} \tag{4.3}$$

and the integrals become

$$\begin{aligned} I_\pm^\mu &= \int_{-\frac{l}{2}}^{\frac{l}{2}} d\sigma_\pm \left(\dot{X}_{\pm 0}^\mu + \ddot{X}_{\pm 0}^\mu \sigma_\pm \right) e^{\frac{i}{12} \omega \ddot{X}_\pm^2 \sigma_\pm^3} \\ &= \dot{X}_{\pm 0}^\mu \frac{l}{2L_\pm} \int_{-L_\pm}^{L_\pm} du \, e^{iu^3} + \ddot{X}_{\pm 0}^\mu \left(\frac{l}{2L_\pm} \right)^2 \int_{-L_\pm}^{L_\pm} du \, u e^{iu^3} \end{aligned} \tag{4.4}$$

where we changed variables:

$$\begin{aligned} u &= \left(\frac{\ddot{X}_{\pm 0}^2 \omega}{12} \right)^{\frac{1}{3}} \sigma_\pm \\ L_\pm &= \left(\frac{\ddot{X}_{\pm 0}^2 \omega}{12} \right)^{\frac{1}{3}} \frac{l}{2} \end{aligned} \tag{4.5}$$

4.1 Reaching the TT-gauge

Before going further, let's fix the remaining gauge freedom. Writing (4.4) as

$$I^{\mu}_{\pm} \equiv \dot{X}^{\mu}_{\pm 0} B_{\pm} + \ddot{X}^{\mu}_{\pm 0} C_{\pm} \tag{4.6}$$

we get

$$\begin{aligned} I^{(\mu}_{+} I^{\nu)}_{-} &= \dot{X}^{(\mu}_{0} \xi^{\nu)} + \ddot{X}^{(\mu}_{+0} \ddot{X}^{\nu)}_{-0} C_{+} C_{-} \\ \xi^{\nu} &\equiv \dot{X}^{\nu}_{0} B_{+} B_{-} + \ddot{X}^{\nu}_{-0} B_{+} C_{-} + \ddot{X}^{\nu}_{+0} B_{-} C_{+} \end{aligned} \tag{4.7}$$

The following coordinate transformation will get rid of the ξ term:

$$\begin{aligned} \varepsilon^{\mu}(x) &= -i \frac{G\mu}{2\pi r} \int d\omega \, e^{ik\cdot x} \frac{\xi^{\mu}(\omega)}{\omega} \\ \varepsilon^{\mu}{}_{,\nu} &= \frac{G\mu}{2\pi r} \int d\omega \, e^{-i\omega(t-r)} \frac{\xi^{\mu} k_{\nu}}{\omega} \end{aligned} \tag{4.8}$$

It is easy to see that this transformation is allowed, i.e. $\Box \varepsilon^{\mu} = 0$ since $k^2 = 0$. Also, our choice of k, $\dot{X}_0{}^2 = 0$ (2.26) and (2.24) imply $\varepsilon^{\mu}{}_{,\mu} = 0$. Then from (3.6) we get

$$\begin{aligned} \bar{h}'^{\mu\nu}(x) &= \frac{2G}{\pi r} \int d\omega \, e^{-i\omega t_R} \frac{\mu}{2} I^{(\mu}_{+} I^{\nu)}_{-} - 2 \left[\frac{G\mu}{2\pi r} \int d\omega \, e^{-i\omega t_R} \dot{X}^{(\mu}_{0} \xi^{\nu)} \right] \\ \bar{h}^{\mu\nu}(\omega, \boldsymbol{x}) &= \frac{2G\mu}{r} \ddot{X}^{(\mu}_{+0} \ddot{X}^{\nu)}_{-0} C_{+} C_{-} \end{aligned} \tag{4.9}$$

Note that the last term in (3.6) in this case is proportional to r^{-2} so we dropped it.

Next, we rotate so that $\boldsymbol{k} = \omega \hat{\boldsymbol{z}}$. Both $\ddot{\mathbf{X}}_{+0}$ and $\ddot{\mathbf{X}}_{-0}$ are now in the xy plane by (2.28) and the metric perturbation takes the form

$$\begin{aligned} \ddot{X}^{(I}_{+0} \ddot{X}^{J)}_{-0} &= \left| \ddot{X}_{+0} \right| \left| \ddot{X}_{-0} \right| \begin{bmatrix} \cos\theta_{+} \cos\theta_{-} & \cos\theta_{(+} \sin\theta_{-)} \\ \cos\theta_{(+} \sin\theta_{-)} & \sin\theta_{+} \sin\theta_{-} \end{bmatrix} \\ &= \frac{1}{2} \left| \ddot{X}_{+0} \right| \left| \ddot{X}_{-0} \right| \begin{bmatrix} \cos(\theta_{+} - \theta_{-}) + \cos(\theta_{+} + \theta_{-}) & \sin(\theta_{+} + \theta_{-}) \\ \sin(\theta_{+} + \theta_{-}) & \cos(\theta_{+} - \theta_{-}) - \cos(\theta_{+} + \theta_{-}) \end{bmatrix} \end{aligned} \tag{4.10}$$

where I and $J = 1, 2$. Rotating again so that the x axis bisects the angle between $\ddot{\mathbf{X}}_{+0}$ and $\ddot{\mathbf{X}}_{-0}$ gives

$$\ddot{X}_{+0}^{(I}\ddot{X}_{-0}^{J)} = \frac{1}{2}\left|\ddot{X}_{+0}\right|\left|\ddot{X}_{-0}\right|\begin{bmatrix}1 & 0\\ 0 & -1\end{bmatrix} + \frac{1}{2}\ddot{X}_{+0}\cdot\ddot{X}_{-0}\begin{bmatrix}1 & 0\\ 0 & 1\end{bmatrix} \tag{4.11}$$

Note that we could also rotate by $\frac{\pi}{4}$ more and it would be the other linear polarization ($\epsilon_{\otimes}^{\mu\nu}$) that would survive. The important point is that there is only one polarization present.

The final step is then to remove the trace by another transformation (3.4) with

$$\begin{aligned}\varepsilon^{\mu}(x) &= -i\frac{G\mu}{2\pi r}\int d\omega\, e^{ik\cdot x}\zeta^{\mu}(\omega) \\ \zeta^{\mu} &\equiv \frac{C_+C_-}{4\omega}\ddot{X}_{+0}\cdot\ddot{X}_{-0}(1,0,0,-1)\end{aligned} \tag{4.12}$$

With $k^{\mu} = \omega(1,0,0,1)$, we find

$$\begin{aligned}\zeta^{\mu}k_{\mu} &= -\tfrac{1}{2}C_+C_-\ddot{X}_{+0}\cdot\ddot{X}_{-0} \\ \zeta^{0}k^{0} &= -\zeta^{3}k^{3} = \tfrac{1}{4}C_+C_-\ddot{X}_{+0}\cdot\ddot{X}_{-0} \\ \zeta^{(0}k^{3)} &= 0\end{aligned} \tag{4.13}$$

Most of the terms in the transformed metric (3.6) cancel and we get rid of the trace term in (4.11). We now have the gravitational wave spectrum in the TT-gauge:

$$\begin{aligned}h^{\mu\nu}(\omega,\boldsymbol{x}) &= \frac{2G\mu}{r}\frac{1}{2}\epsilon_{\oplus}^{\mu\nu}\left|\ddot{X}_{+0}\right|\left|\ddot{X}_{-0}\right|C_+C_- \\ &= \epsilon_{\oplus}^{\mu\nu}\frac{G\mu}{r}\left|\ddot{X}_{+0}\right|\left|\ddot{X}_{-0}\right|\left(\frac{l}{2}\right)^4 L_+^{-2}\int_{-L_+}^{L_+}du\,ue^{iu^3}L_-^{-2}\int_{-L_-}^{L_-}du\,ue^{iu^3}\end{aligned} \tag{4.14}$$

where $\epsilon_{\oplus}^{\mu\nu}$ is the polarization tensor (3.13).

The presence of $\left(\frac{l}{2}\right)^4$ suggests that we should express all lengths in units of $\frac{l}{2}$ and we shall do it from this point on. Then, $r^{-1}\left|\ddot{X}_{+0}\right|\left|\ddot{X}_{-0}\right|$ absorbs 3 powers and the remaining one goes into $h(\omega,\boldsymbol{x})$ ($h(x)$ is dimensionless, but the Fourier transform contains the measure

dt). Similarly, there is one factor of $\frac{l}{2}$ in $L_{\pm}$ (4.5) and it is absorbed by $\ddot{X}_{\pm 0}^{\frac{2}{3}}$ and $|\omega|^{\frac{1}{3}}$. To simplify things further, we define a normalized metric and frequency

$$\begin{aligned} \tilde{h}\left(\tilde{\omega}, \boldsymbol{x}\right) &\equiv \frac{r}{G\mu \left|\ddot{X}_{+0}\right| \left|\ddot{X}_{-0}\right|} h^{11}\left(\omega, \boldsymbol{x}\right) \\ \tilde{\omega} &\equiv \frac{\left|\ddot{X}_{+0}\right| \left|\ddot{X}_{-0}\right|}{12} \omega \end{aligned} \tag{4.15}$$

The only remaining parameter is then the ratio of the + and - acceleration components at the cusp

$$a \equiv \frac{\left|\ddot{X}_{+0}\right|}{\left|\ddot{X}_{-0}\right|} \tag{4.16}$$

The spectrum 4.14 is then

$$\begin{aligned} \tilde{h}\left(\tilde{\omega}, \boldsymbol{x}\right) &= \tilde{\omega}^{-\frac{4}{3}} J\left(a\tilde{\omega}\right) J\left(a^{-1}\tilde{\omega}\right) \\ J\left(w\right) &\equiv \int_{-w^{\frac{1}{3}}}^{w^{\frac{1}{3}}} du\, u e^{iu^3} \end{aligned} \tag{4.17}$$

4.2 Spectrum

We now solve the integral $J\left(w\right)$. Note that the symmetrical limits and antisymmetric u will only pick the antisymmetric part of the exponential: $i \sin\left(u^3\right)$. This integral can be expressed in terms of hypergeometric functions ${}_pF_q\left(\cdots\,;\,\cdots\,;\,z\right)$ [22], the incomplete gamma

function $\Gamma(a,z)$ [23] or the exponential integral function $E_\nu(z)$ [24]:

$$\begin{aligned} J(w) &= 2\int_0^{w^{\frac{1}{3}}} du\, u \sin u^3 \\ &= \frac{1}{2} i w^{\frac{2}{3}} \left[{}_1F_1\left(\frac{3}{2};\frac{5}{3};-iw\right) - {}_1F_1\left(\frac{3}{2};\frac{5}{3};iw\right)\right] \\ &= \frac{1}{3} i \left[\left(\tfrac{1}{2}+\tfrac{\sqrt{3}}{2}i\right)\Gamma\left(\frac{2}{3},-iw\right) - \left(\tfrac{1}{2}-\tfrac{\sqrt{3}}{2}i\right)\Gamma\left(\frac{2}{3},iw\right)\right] + \frac{1}{\sqrt{3}}\Gamma\left(\frac{2}{3}\right) \\ &= \frac{1}{3} i w^{\frac{2}{3}} \left[E_{\frac{1}{3}}(-iw) - E_{\frac{1}{3}}(iw)\right] + \frac{1}{\sqrt{3}}\Gamma\left(\frac{2}{3}\right) \end{aligned} \tag{4.18}$$

Figure 4.1 shows that the integral tends to a constant at high frequencies and that low frequencies are suppressed. Two examples of the spectrum are shown in figure 4.2, for $a = 1$ and 1.8. The dotted line is the approximate solution, when taking only then constant piece in the integrals ($J(\infty) = \frac{1}{\sqrt{3}}\Gamma\left(\frac{2}{3}\right)$). To use this approximation, we need to introduce a cut-off at low frequencies since the spectrum amplitude diverges. In figure 4.1 we see that the amplitude drops at $w \approx 1$ so we should impose $|\omega| \geq \frac{12}{\ddot{X}^2_{\pm 0}}$.

4.3 Wave profile

If we want to study the shape of the wave, we have to take the inverse Fourier transform of the spectrum. To be consistent with our variables (4.15), we also define a normalized retarded time such that $\tilde{\omega}\tilde{t}_R = \omega t_R$. The normalized metric is then

$$\begin{aligned} \tilde{h}\left(\tilde{t}_R\right) &\equiv \int \frac{d\tilde{\omega}}{2\pi} e^{-i\tilde{\omega}\tilde{t}_R} \tilde{h}\left(\tilde{\omega}, \boldsymbol{x}\right) \\ &= \frac{r}{G\mu \left|\ddot{X}_{+0}\right| \left|\ddot{X}_{-0}\right|} \int \frac{d\tilde{\omega}}{2\pi} e^{-i\tilde{\omega}\tilde{t}_R} h\left(\omega, \boldsymbol{x}\right) \\ &= \frac{r}{12 G\mu} \int \frac{d\omega}{2\pi} e^{-i\omega t_R} h\left(\omega, \boldsymbol{x}\right) \\ &= \frac{r}{12 G\mu} h\left(t_R, \boldsymbol{x}\right) \end{aligned} \tag{4.19}$$

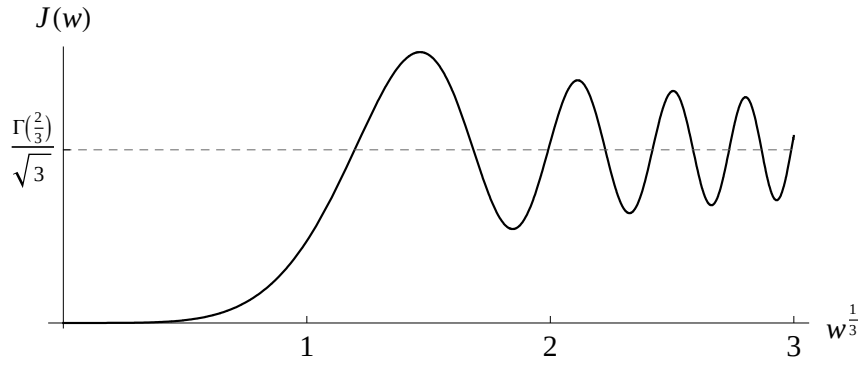

Figure 4.1: Graph of the integral (4.18): $I = 2\int_0^L du\, \sin u^3$, a factor in the expression of the gravitational wave spectrum far from an idealised string cusp. The bound L is proportional to the string length and depends on the wave frequency as $\omega^{\frac{1}{3}}$.

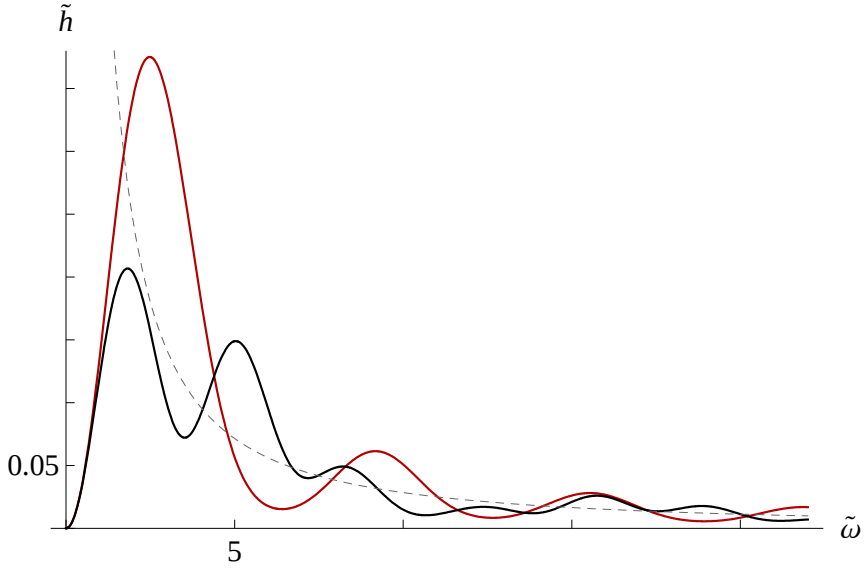

Figure 4.2: Gravitational wave spectrum from an idealised string cusp in the TT-gauge, for $\left|\ddot{X}_{+0}\right| : \left|\ddot{X}_{-0}\right| = 1$ (red) or 1.8 (black). The dotted line shows the $\omega^{-\frac{4}{3}}$ approximation, which needs to be cut off at low frequencies.

Unfortunately, that integral is too complex to be evaluated in terms of known functions. It is however possible to calculate it explicitly from equation (3.23), without going to Fourier space. This is done in appendix B, giving a piecewise function containing hypergeometric functions. The other option is to compute the wave profile numerically either by numerical integration or much more efficiently by discrete Fourier transform. We used *Mathematica* to compute and plot some examples for different values of a. These are shown in figure 4.3.

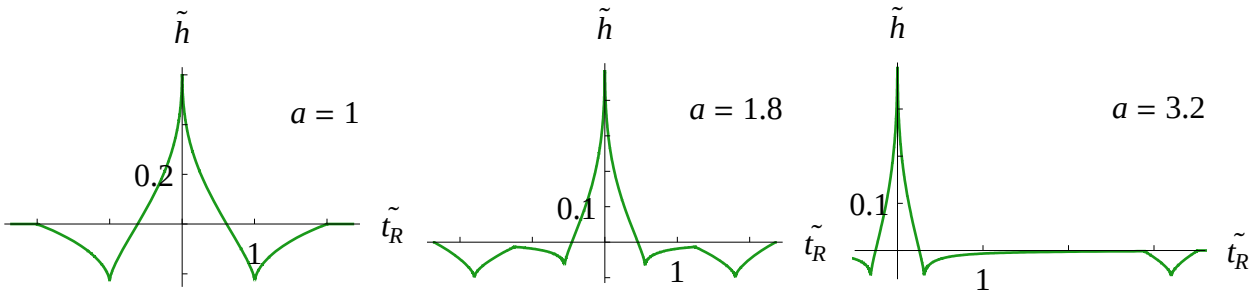

Figure 4.3: Gravitational wave spectrum from an idealised string cusp in the TT-gauge, for different values of $a \equiv \left|\ddot{X}_{+0}\right| / \left|\ddot{X}_{-0}\right|$.

To better understand this wave shape, we can look at which points of the worldsheet participate in producing the wave at a specific retarded time. From our approximation (3.24), we find that the points that participate are those that satisfy

$$t_R = X^0 - X^3 \tag{4.20}$$

In figure 4.4, we show the patch of the worldsheet that is used when computing the wave profile. Recall that we used a square region in $\sigma_+\sigma_-$ coordinates. On the worldsheet, lines that satisfy (4.20) for different retarded times are displayed. The color of each of these source lines allows us to find the corresponding point on the wave profile, also shown in the

figure. This particular case is for $a = 1.8$. Note also that the color (gray scale) of the 3d worldsheet indicates the relative speed of the string at that point, a lighter color indicating faster motion.

The most obvious feature of the wave profile is the many singular (non smooth) points. However, studying the matching source lines shows that only the main peak at $t_R = 0$ is a physical effect, the others being due to the edges of our patch. We see that we first detect the perturbation produced by a corner and then extending along one edge until we reach another corner ($\tilde{t}_R \approx \pm 1.2$). The other four singular points are harder to explain. Careful examination of the worldsheet in 3d shows that they correspond to moments when an edge of the source line starts having a speed in an opposite direction as before (in the plane perpendicular to $\dot{\mathbf{X}}_0$), apparently changing abruptly the total quadrupole moment of the source line. In any case, none of these would be present in a realistic scenario. It will be useful to compare this figure with the more complicated cases later.

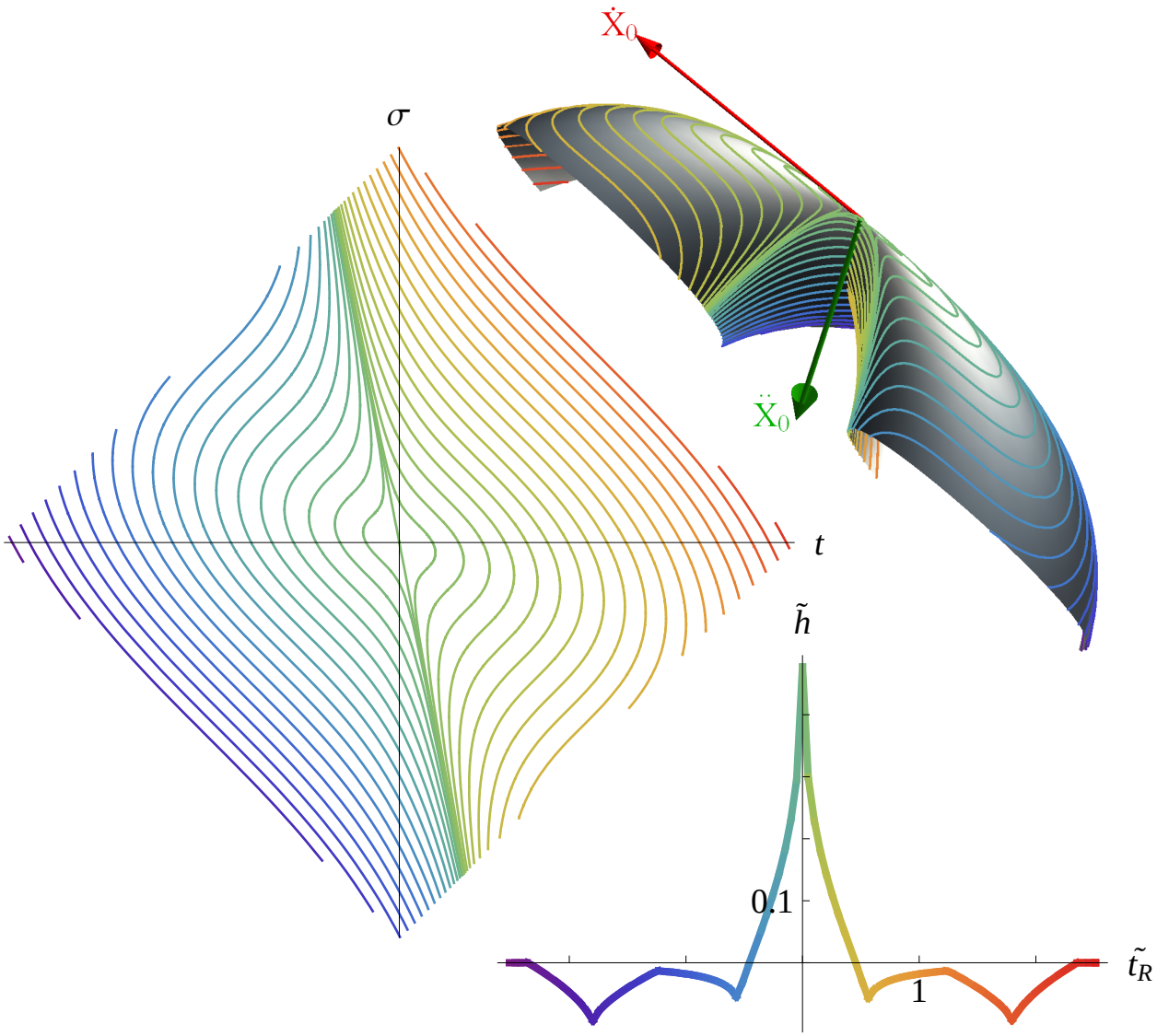

Figure 4.4: Comparison of the wave profile and its source. Top right: Shape of the worldsheet patch that was used as the source. The darker areas correspond to slower string speed. Left: Same patch in worldsheet coordinates. Lower right: Corresponding wave profile. Each color corresponds to a specific retarded time so we can identify the (linear) regions on the worldsheet that produce a specific point of the wave.

5. Lorentz violation

Let us briefly consider the fate of Lorentz symmetry in quantum gravity research. The different approaches to the quantum gravity problem can be associated with three areas of theoretical physics [25]: particle physics, general relativity and more recently condensed matter physics, each adopting a different view on Lorentz symmetry. From the particle physics perspective, the exact symmetry is a feature of the classical spacetime background. Still, there can be spontaneous symmetry breaking and this has been studied for example in string theory [26]. The general relativity perspective, which includes loop quantum gravity and noncommutative spacetimes, instead rejects the idea of a background spacetime and attempts to describe it in a way that incorporates the fundamental limitations on measurements. In loop quantum gravity, the fate of Lorentz symmetry is still uncertain, but recently the attention has shifted towards the possibility of a broken or deformed symmetry. In noncommutative spacetimes, the symmetries are in general described using the structure of Hopf algebras instead of Lie algebras and one expects Lorentz symmetry to be broken (or perhaps deformed in special cases). Finally, from the condensed matter perspective, some properties of spacetime including Lorentz symmetry are viewed as being only approximate or "emergent", in the same sense that some collective degrees of freedom of a system can be relevant only near a critical point [27].

To clarify what is meant by a deformed rather than broken symmetry, consider the so-called doubly special relativity theory [28, 29], where we introduce a new observer independent high energy scale, usually taken to be the Planck scale. We then have a different (exact) symmetry that resembles Lorentz symmetry at low energies.

5.1 Effective field theory and the standard model extension

Effective field theory is a good starting point to study Lorentz violation. It offers a framework that is very flexible, seemingly able to describe any theory that is local and invariant under local spacetime translation above some length scale. It also allows for clear predictions and it can be constrained by experiment. The standard model and general relativity can be considered effective field theories, as well as condensed matter systems at appropriate scales and even string theory. On the other hand, there are some effects that are not describable in this framework [30], such as stochastic fluctuations or a "foamy" spacetime structure at very small scales. Non-commutative geometry can also lead to problematic UV/IR mixing. Still, any realistic theory, regardless of high energy effects, must allow an effective field theory description at low energies, given the success of current theories.

To study Lorentz violation in the context of effective field theory, we must introduce new tensors that break the Lorentz symmetry. If they are kept constant (explicit violation), we find that the energy-momentum tensor is not conserved and the Einstein equations are inconsistent, except for very specific solutions. Still, in the flat space limit, where gravitational effects are negligible, or if we chose to investigate those specific solutions, this approach can be useful. Such a theory in flat space has been derived that includes all possible renormalizable Lorentz violating terms that can be added to the standard model without changing the field content or violating the gauge symmetry, the so-called (minimal) Standard Model Extension (SME) [31]. This framework has been further developed, incorporating a gravity sector with Riemann-Cartan geometry and gravitational couplings in the matter and gauge sectors [32].

Before looking in more detail at the pure gravity sector, we would like to mention an

important issue with Lorentz violating effective field theories: why do they have such a good approximate Lorentz symmetry at low energies? [33, 34] The Lorentz violating renormalizable operators are already severely constrained. We might be tempted to consider higher dimension operators that would be naturally suppressed by inverse powers of the Plank mass, but without a symmetry that would forbid lower dimension operators, they would be generated by radiative corrections and imply strong Lorentz violation at low energies. It has been suggested that broken supersymmetry with CPT symmetry or a braneworld scenario might resolve the issue. Doubly special relativity also evades many constraints since it has no preferred frame and thus might be more appealing phenomenologically. In any case, this fine-tuning issue requires further attention.

The pure gravity sector of the SME is defined using the tetrad (or vierbein) formalism, the natural language for coupling gravity to fermions. The fundamental degrees of freedom are contained in the tetrad, a (pseudo) orthonormal basis of vectors $\boldsymbol{e}_a = e^{\mu}{}_a \partial_\mu$ with dual basis $\theta^a = e_\mu{}^a dx^\mu$ such that

$$e^{\mu}{}_a e_\nu{}^a = \delta^\mu_\nu, \quad e^{\mu}{}_a e_\mu{}^b = \delta^b_a \tag{5.1}$$

$$g_{\mu\nu} = e^a_\mu e^b_\nu \eta_{ab} \tag{5.2}$$

In Riemann-Cartan geometry, the connection one-form $\omega^b{}_a = \Gamma^b_{ca}\theta^c$ is independent of the tetrad and allows for non-zero torsion; in Einstein-Cartan theory (general relativity with torsion), this is the case only in the presence of an intrinsic spin density of matter. In realistic situations, torsion effects are typically heavily suppressed compared to curvature effects and we will only consider the Riemannian limit, with zero torsion. The low energy action in this case is

$$S = \frac{1}{16\pi G} \int d^4x\, e \left[(1-q)\, R - 2\Lambda + s^{\mu\nu} R_{\mu\nu} + t^{\kappa\lambda\mu\nu} R_{\kappa\lambda\mu\nu} \right] \tag{5.3}$$

where e is the determinant of the tetrad, Λ is the cosmological constant and the coefficients s and t have the symmetries of the Ricci and Riemann tensors respectively. They are

also defined as traceless (otherwise the traces can be absorbed in q and s). There are 19 independent Lorentz violating degrees of freedom.

But again, having these coefficient fixed places very limiting conditions on them if we want a conserved energy-momentum tensor. To retain the general solutions, we must instead take them as dynamic objects. Energy-momentum conservation is then a result of the diffeomorphism invariant action. If the new tensors also have a potential that gives them a non-zero vacuum expectation value, Lorentz symmetry is spontaneously broken. Our main interest will be one such theory, most often called Einstein-aether theory.

6. Einstein-aether theory

Einstein-aether theory is a theory of gravity with dynamic preferred frame [35]. It introduces a single new dynamic timelike vector field u^μ, called the aether. By encoding the Lorentz violation with this aether field and the metric, the theory preserves rotational invariance. The most general action that is diffeomorphism invariant and quadratic in derivatives of the aether and metric is

$$\begin{aligned} S &= \frac{1}{16\pi G}\int d^4x\,\sqrt{-g}\left[R + K^{\mu\nu}{}_{\alpha\beta}\nabla_\mu u^\alpha \nabla_\nu u^\beta + V\left(u^\alpha u_\alpha\right)\right] \\ K^{\mu\nu}{}_{\alpha\beta} &\equiv c_1 g^{\mu\nu}g_{\alpha\beta} + c_2\delta^\mu_\alpha\delta^\nu_\beta + c_3\delta^\mu_\beta\delta^\nu_\alpha + c_4 u^\mu u^\nu g_{\alpha\beta} \end{aligned} \tag{6.1}$$

The c_i coefficients are dimensionless constants[2]. Compared with the SME gravity action, here $q = \Lambda = 0$ and integrating by parts the s term gives the c_2 and c_3 terms. The potential V imposes a non-zero vacuum expectation value. However, the theory is unstable (negative energies associated with u^0) unless the potential is a strict constraint of the form $\lambda\left(u^\alpha u_\alpha - v^2\right)$ where λ is a Lagrange multiplier, or in the special case $c_1 + c_2 + c_3 = 0$ [36]. The constraint removes a degree of freedom, leaving a positive definite Hamiltonian but also making the theory non-renormalizable and valid only semi-classically (at tree level). Since the length of u is extra information not needed to specify a preferred frame, we will fix $v^2 = 1$ by rescaling u. Then small Lorentz violation at low energies translates to small

[2]Note that all cited work in which these coefficients appear used the signature $(+,-,-,-)$ instead of $(-,+,+,+)$ that we use here so there will be sign differences when comparing with our calculations. In particular, since the c_4 term includes the metric, our c_4 is the opposite of theirs. Unfortunately, there are many other sign differences whose sources are not as easy to isolate. We chose to copy the constraints in section 5.3 and other relations of these parameters (e.g. 6.2) as they appear in the cited work, so again we cannot compare these directly with our results.

kinetic coefficients c_i. We could instead rescale u such that the coefficients are of order 1, then it is the size of the vacuum expectation value for u that would be constrained.

We will derive the field equations by varying with respect to the metric, the aether and the Lagrange multiplier. Note that we choose the most traditional (Einstein-Hilbert) action for general relativity, where the fundamental variable is the metric which uniquely defines the torsion-free connection. However, there are many other actions for general relativity that use different fundamental variables and that are equivalent at the classical level [37]. They would not all be equivalent in the case of Einstein-aether theory. For example, in the Palatini formulation, the spin connection is varied independently from the tetrad. In general relativity its equation of motion gives zero torsion, but here the covariant derivatives of the aether would introduce additional terms, giving non-zero torsion and indicating a different theory. Such a theory has not yet been investigated.

It has been noted [38, 39] that if the parameters satisfy

$$\begin{aligned} c_1 + c_4 &= c_1 + c_2 + c_3 = 0 \\ c_3 &= \pm\sqrt{c_1\,(c_1 - 2)} \\ c_1 &\leq 0 \end{aligned} \tag{6.2}$$

then the theory in vacuum is equivalent to general relativity by a field redefinition of the form

$$g'_{\mu\nu} = g_{\mu\nu} + (1 - B)\, u_\mu u_\nu \tag{6.3}$$

where $B > 0$ in order for g' to have Lorentzian signature. It is also possible to redefine the fields such that $c_1 + c_3 = 0$. Combined with the previous result, the theory in vacuum would then be equivalent to general relativity if all c_i's vanish [35]. These results have been obtained by considering a specific type of field redefinition depending on two parameters and there might be other ways to relate the theory to general relativity. Thus the claim

that non-zero coefficients when $c_1 + c_3 = 0$ ensure true deviation from general relativity [35] isn't obviously true. In any case, once we consider the theory with matter, we are no longer free to redefine the metric (to which the matter couples) and Lorentz violating effects are present.

6.1 Field equations

We now derive the field equations from the following action:

$$\begin{aligned} S &= \frac{1}{16\pi G}\int d^4x\,\sqrt{-g}\,(R+\mathcal{L}_u) \\ \mathcal{L}_u &= K^{\mu\nu}{}_{\alpha\beta}\nabla_\mu u^\alpha \nabla_\nu u^\beta + \lambda\,(u^\alpha u_\alpha + 1) \\ K^{\mu\nu}{}_{\alpha\beta} &\equiv c_1 g^{\mu\nu}g_{\alpha\beta} + c_2\delta^\mu_\alpha\delta^\nu_\beta + c_3\delta^\mu_\beta\delta^\nu_\alpha + c_4 u^\mu u^\nu g_{\alpha\beta} \end{aligned} \tag{6.4}$$

First, varying the Lagrange parameter enforces the constraint: $u^\alpha u_\alpha = -1$. Next, varying the aether we get

$$\begin{aligned} \frac{\delta\mathcal{L}_u}{\delta u^\mu} &= 2\lambda u_\mu + 2c_4 u_{\alpha;\mu}u^\alpha{}_{;\beta}u^\beta - 2\left(K^{\alpha\beta}{}_{\mu\nu}u^\nu{}_{;\beta}\right)_{;\alpha} \\ 0 &= \lambda u_\mu + c_4\left(u_{\alpha;\mu}u^\alpha{}_{;\beta} - 2u_{\mu;(\beta}u^\alpha{}_{;\alpha)}\right)u^\beta - K^{\alpha\beta}{}_{\mu\nu}u^\nu{}_{;\beta\alpha} \\ \lambda &= -K^{\alpha\beta}{}_{\mu\nu}u^\mu u^\nu{}_{;\beta\alpha} + c_4 u^\alpha u^\beta\left(u_{[\lambda;\alpha]}u^\lambda{}_{;\beta} - u_{\alpha;\beta}u^\lambda{}_{;\lambda}\right) \end{aligned} \tag{6.5}$$

As in general relativity (e.g. [20] chapter 21), we can carry the variation with respect to the metric in a frame where $\Gamma^\lambda_{\mu\nu} = 0$ and then substitute covariant derivatives for ordinary derivatives to recover the general formula. The variation of the scalar curvature is then

$$\delta R = \delta g^{\mu\kappa}R_{\mu\kappa} + g^{\mu\kappa}\delta R^\lambda{}_{\mu\lambda\kappa} = \delta g^{\mu\kappa}R_{\mu\kappa} + 2g^{\mu\kappa}\delta\Gamma^\lambda_{\mu[\kappa;\lambda]} \tag{6.6}$$

Integrating by parts the $\delta\Gamma$ term will give it a zero coefficient (in the form of covariant derivatives of the metric and its determinant). We then obtain the familiar form for Einstein's

equation, with an aether dependant energy-momentum tensor.

$$G_{\mu\nu} = T_{\mu\nu} = \frac{1}{2} g_{\mu\nu} \mathcal{L}_u - \frac{\delta \mathcal{L}_u}{\delta g^{\mu\nu}} \tag{6.7}$$

In the presence of other matter fields ϕ, we get instead

$$G_{\mu\nu} - T_{\mu\nu}\left(u\right) = 8\pi G T_{\mu\nu}\left(\phi\right) \tag{6.8}$$

The variation of the aether Lagrangian with respect to the metric is

$$\begin{aligned} \frac{\delta \mathcal{L}_u}{\delta g^{\mu\nu}} &= -\lambda u_\mu u_\nu + c_1 g^{\alpha\beta} u_{\alpha;\mu} u_{\beta;\nu} - \left(c_1 g^{\alpha\beta} + c_4 u^\alpha u^\beta\right) u_{\mu;\alpha} u_{\nu;\beta} \\ &\quad + K^{\rho\sigma}{}_{\alpha\beta} \left(u^\alpha{}_{;\rho} \frac{\delta \Gamma^\beta_{\sigma\lambda}}{\delta g^{\mu\nu}} + u^\beta{}_{;\sigma} \frac{\delta \Gamma^\alpha_{\rho\lambda}}{\delta g^{\mu\nu}} \right) u^\lambda \end{aligned} \tag{6.9}$$

where the minus signs come from $\delta g_{\alpha\beta} = -g_{\alpha\mu} g_{\beta\nu} \delta g^{\mu\nu}$. Since $K^{\rho\sigma}{}_{\alpha\beta}$ is invariant under the exchange of α, ρ with β, σ, both $\delta\Gamma$ terms are equal. Using again a frame where the connection coefficients vanish, we find

$$\begin{aligned} \delta\Gamma^\beta_{\sigma\lambda} &= \frac{1}{2} g^{\beta\tau} \left(\delta^\xi_\sigma \delta^\zeta_\tau \delta^\kappa_\lambda + \delta^\xi_\tau \delta^\zeta_\lambda \delta^\kappa_\sigma - \delta^\xi_\lambda \delta^\zeta_\sigma \delta^\kappa_\tau \right) \delta g_{\xi\zeta;\kappa} \\ &= -\frac{1}{2} \left(g_{\sigma\mu} \delta^\beta_\nu \delta^\kappa_\lambda + \delta^\beta_\mu g_{\lambda\nu} \delta^\kappa_\sigma - g_{\lambda\mu} g_{\sigma\nu} g^{\beta\kappa} \right) \left(\delta g^{\mu\nu}\right)_{;\kappa} \end{aligned} \tag{6.10}$$

Then integrating by parts, the K factor becomes

$$\left(K^{\rho\sigma}{}_{\alpha\beta} u^\alpha{}_{;\rho} u^\lambda\right)_{;\kappa} = \left[c_4 \left(u^\rho{}_{;\kappa} u^\sigma + u^\rho u^\sigma{}_{;\kappa} \right) u_{\beta;\rho} u^\lambda + K^{\rho\sigma}{}_{\alpha\beta} \left(u^\alpha{}_{;\rho\kappa} u^\lambda + u^\alpha{}_{;\rho} u^\lambda{}_{;\kappa} \right) \right] \tag{6.11}$$

Expanding everything and keeping only the symmetric part in $\mu\nu$ for the field equation (since the metric is symmetric), we get

$$\begin{aligned} T_{\mu\nu} &= \frac{1}{2} g_{\mu\nu} K^{\kappa\lambda}{}_{\alpha\beta} u^\alpha{}_{;\kappa} u^\beta{}_{;\lambda} - c_1 \left[\left(u_{(\mu;\nu)} u^\alpha - u^\alpha{}_{;(\mu} u_{\nu)} \right)_{;\alpha} + g^{\alpha\beta} u_{\alpha;\mu} u_{\beta;\nu} \right] \\ &\quad - c_2 \left[g_{\mu\nu} \left(u^\alpha{}_{;\alpha} u^\beta \right)_{;\beta} - u^\alpha{}_{;\alpha(\mu} u_{\nu)} \right] - c_3 \left[\left(u_{(\mu;\nu)} u^\alpha \right)_{;\alpha} + u^\alpha{}_{;(\mu} u_{\nu);\alpha} - g^{\alpha\beta} \left(u_{(\mu} u_{\nu);\beta} \right)_{;\alpha} \right] \\ &\quad - c_4 \left[u_{\alpha;(\mu} u_{\nu)} u^\alpha{}_{;\beta} u^\beta + \left(u_{(\mu} u_{\nu);\alpha} u^\alpha u^\beta - u_\mu u_\nu u^\alpha u^\beta{}_{;\alpha} \right)_{;\beta} \right] \end{aligned} \tag{6.12}$$

where we have substituted for λ using the other field equations.

6.2 Wave modes

Next we find the linearized field equations about a flat background $\eta_{\mu\nu} = (-1, 1, 1, 1)$ and constant aether $w^\alpha = (1, 0, 0, 0)$:

$$\begin{aligned} g_{\mu\nu} &= \eta_{\mu\nu} + h_{\mu\nu} \\ u^\alpha &= w^\alpha + v^\alpha \end{aligned} \tag{6.13}$$

To first order in the perturbations $h_{\mu\nu}$ and v^α, the λ field equations becomes

$$\begin{aligned} 2\eta_{\mu\nu} w^\mu v^\nu + g_{\mu\nu} w^\mu w^\nu &= -1 \\ 2v^0 + h_{00} &= 0 \\ 2v_0 &= h_{00} \end{aligned} \tag{6.14}$$

We find that λ is first order in the perturbations,

$$\lambda = c_1 \eta^{\alpha\beta} u^0{}_{;\alpha\beta} - c_2 u^\alpha{}_{;\alpha 0} - c_3 u^\alpha{}_{;0\alpha} + c_4 u^0{}_{;00} \tag{6.15}$$

so the uncontracted form of the aether field equation (6.5) becomes

$$0 = \mathcal{V}_\mu \equiv -\lambda w_\mu + c_1 \eta^{a\beta} u_{\mu;\alpha\beta} + c_2 u^\alpha{}_{;\alpha\mu} + c_3 u^\alpha{}_{;\mu\alpha} + c_4 u_{\mu;00} \tag{6.16}$$

Finally, the metric equations are

$$\begin{aligned} \mathcal{G}_{\mu\nu} &\equiv G^{(1)}_{\mu\nu} - T^{(1)}_{\mu\nu} \\ &= -2\eta^{\kappa\lambda} h_{\llcorner \kappa \ulcorner \lambda, \mu \lrcorner \nu \urcorner} + \eta_{\mu\nu} \eta^{\alpha\beta} \eta^{\kappa\lambda} h_{\llcorner \kappa\lambda, \alpha \lrcorner \beta} \\ &\quad + c_1 \left(u_{(\mu;\nu)0} - u^\alpha{}_{;(\mu\alpha} w_{\nu)} \right) + c_2 \left(\eta_{\mu\nu} u^\alpha{}_{;\alpha 0} - u^\alpha{}_{;\alpha(\mu} w_{\nu)} \right) \\ &\quad + c_3 \left(u_{(\mu;\nu)0} - \eta^{\alpha\beta} w_{(\mu} u_{\nu);\beta\alpha} \right) + c_4 \left(w_{(\mu} u_{\nu);00} - w_\mu w_\nu u^\alpha{}_{;0\alpha} \right) \\ &= -2\eta^{\kappa\lambda} h_{\llcorner \kappa \ulcorner \lambda, \mu \lrcorner \nu \urcorner} + \eta_{\mu\nu} \eta^{\alpha\beta} \eta^{\kappa\lambda} h_{\llcorner \kappa\lambda, \alpha \lrcorner \beta} \\ &\quad + w_{(\mu} \left[-c_1 u^\alpha{}_{;\nu)\alpha} - c_2 u^\alpha{}_{;\alpha\nu)} - c_3 \eta^{\alpha\beta} u_{\nu);\beta\alpha} + c_4 u_{\nu);00} \right] \\ &\quad + c_2 \eta_{\mu\nu} u^\alpha{}_{;\alpha 0} + (c_1 + c_3) u_{(\mu;\nu)0} - c_4 w_\mu w_\nu u^\alpha{}_{;0\alpha} \end{aligned} \tag{6.17}$$

where the second derivatives of the aether are taken to first order:

$$\begin{aligned}\left(u^{\lambda}{}_{;\alpha\beta}\right)^{(1)} &= \left(v^{\lambda}{}_{,\alpha} + \Gamma^{\lambda}_{\alpha\kappa} w^{\kappa}\right)_{,\beta} \\ &= v^{\lambda}{}_{,\alpha\beta} + \frac{1}{2}\eta^{\lambda\gamma}\left(h_{\gamma\kappa,\alpha\beta} + h_{\gamma\alpha,\kappa\beta} - h_{\kappa\alpha,\gamma\beta}\right) w^{\kappa} \\ &= \frac{1}{2}\eta^{\lambda\gamma}\left(2v_{\gamma,\alpha\beta} + h_{\gamma 0,\alpha\beta} + h_{\gamma\alpha,0\beta} - h_{0\alpha,\gamma\beta}\right)\end{aligned} \tag{6.18}$$

We now have 15 unknowns (10 components of h, 4 of v and λ) and 15 field equations relating them, but the Bianchi identity (and energy-momentum conservation) reduces the number of independent relations by 4 and we have the usual gauge freedom. Also, we find that the expressions for $2\eta^{\mu\nu}\mathcal{G}_{i\mu;\nu}$ and $\mathcal{V}_{i;0}$ are equal. The relation

$$2\eta^{\mu\nu}\mathcal{G}_{i\mu;\nu} = \mathcal{V}_{i;0} \tag{6.19}$$

is obvious since the left side is zero by the Bianchi identities and energy-momentum conservation and the right side by the aether field equations, but since the actual expressions are equal, this means that the aether field equations are redundant. Having no interest in the value of λ, we also disregard the equation $\mathcal{V}_0 = 0$ and we are left with the 11 equations (6.17) and (6.14).

In previous work [40], the wave modes were found using the following gauge which was shown to be reachable by a coordinate transformation.

$$\begin{aligned} h_{0i} &= 0 \\ v_{i,i} &= 0 \end{aligned} \tag{6.20}$$

Instead, since we are only interested here in the gravitational waves, we will use the preferred frame picked by the aether field, i.e. we impose the conditions

$$v^{\mu} = 0 \tag{6.21}$$

Note that there is residual gauge freedom. Any constant coordinate transformation ((3.4) with $\varepsilon^{\mu}{}_{,0} = 0$) is still allowed. With equation (6.14), this gauge choice implies $h_{00} = 0$, leaving 10 equations for the remaining 9 components of h.

In this gauge and in vacuum, (6.17) becomes

$$\begin{aligned} 0 &= 2\mathcal{G}_{\mu\nu} \qquad (6.22)\\ &= -h_{aa,\mu\nu} + 2\left(h_{a(\mu,\nu)a} - h_{0(\nu,\mu)0}\right) - h_{\mu\nu,aa} + \eta_{\mu\nu}\left(h_{aa,bb} - h_{aa,00} - h_{ab,ba} + 2h_{a0,0a}\right)\\ &\quad + w_{(\mu}\left[2\left(c_3 + c_4\right)h_{\nu)0,00} - \left(c_1 + c_3\right)h_{\nu)a,a0} + \left(c_1 - c_3\right)\left(h_{\nu)0,aa} - h_{0a,a\nu)}\right) - c_2 h_{aa,0\nu)}\right]\\ &\quad - 2c_4 w_\mu w_\nu h_{0a,a0} + c_2\eta_{\mu\nu}h_{aa,00} + \left(1 + c_1 + c_3\right)h_{\mu\nu,00} \end{aligned}$$

The equation for each component can be further simplified:

$$\begin{aligned} 2\mathcal{G}_{00} &= 2\left(c_1 - c_4\right)h_{0a,a0} - h_{aa,bb} + h_{ab,ba} \qquad (6.23)\\ 4\mathcal{G}_{0i} &= 2\left(c_1 - c_4\right)h_{i0,00} + \left(c_2 - 2\right)h_{aa,0i}\\ &\quad + \left(2 + c_1 + c_3\right)h_{ia,a0} + \left(2 + c_1 - c_3\right)\left(h_{0a,ai} - h_{i0,aa}\right)\\ 2\mathcal{G}_{ij} &= \left(1 + c_1 + c_3\right)h_{ij,00} + \eta_{ij}\left[-\left(1 + c_2\right)h_{aa,00} + h_{aa,bb} - h_{ab,ba} + 2h_{a0,0a}\right]\\ &\quad - h_{aa,ij} + h_{aj,ia} - h_{ij,aa} + h_{ia,aj} - 2h_{0(i,j)0} \end{aligned}$$

Then assuming a plane wave solution

$$\begin{aligned} h_{\mu\nu} &= \epsilon_{\mu\nu}e^{ik\cdot x} \qquad (6.24)\\ k &= \left(k_0 \equiv sk_3, 0, 0, k_3\right) \end{aligned}$$

we find the following set of equations

$$\begin{aligned}
\mathcal{G}_{12} &: \; 0 = (1 + c_1 + c_3)\,\epsilon_{12} s^2 - \epsilon_{12} \\
\mathcal{G}_{11} - \mathcal{G}_{22} &: \; 0 = (1 + c_1 + c_3)\,(\epsilon_{11} - \epsilon_{22})\, s^2 - (\epsilon_{11} - \epsilon_{22}) \\
\mathcal{G}_{0I} &: \; 0 = 2\,(c_1 - c_4)\,\epsilon_{0I} s^2 + (2 + c_1 + c_3)\,\epsilon_{I3} s - (2 + c_1 - c_3)\,\epsilon_{0I} \\
\mathcal{G}_{I3} &: \; 0 = (1 + c_1 + c_3)\,\epsilon_{I3} s - \epsilon_{0I} \\
\mathcal{G}_{II} &: \; 0 = (c_1 + c_2 + c_3)\,\epsilon_{II} s^2 - (1 + c_2)\,(\epsilon_{II} + 2\epsilon_{33})\, s^2 + \epsilon_{II} + 4\epsilon_{03} s \\
\mathcal{G}_{33} &: \; 0 = (c_1 + c_2 + c_3)\,\epsilon_{33} - (1 + c_2)\,\epsilon_{II} \\
\mathcal{G}_{00} &: \; 0 = 2\,(c_1 - c_4)\,\epsilon_{03} s - \epsilon_{II}
\end{aligned} \tag{6.25}$$

where I takes the values 1 and 2. As expected since we had an overdetermined system, we find that one more equation is redundant: the expression for $2\mathcal{G}_{03}$ is the same as $\mathcal{G}_{33} s^{-1} + \mathcal{G}_{00} s$. From this system we find 5 independent wave modes with distinct polarizations. The two usual transverse traceless (spin 2) modes are still there, but their speed s is no longer the speed of light, although it is in the limit of small coefficients c_i:

$$\begin{aligned}
&\epsilon_{12} \\
\epsilon_{11} &= -\epsilon_{22} \\
s^2 &= \frac{1}{1 + c_1 + c_3} \to 1
\end{aligned} \tag{6.26}$$

Then there are two traceless (spin 1) modes involving both the propagation direction and time:

$$\begin{aligned}
\epsilon_{I0} &= (1 + c_1 + c_3)\, s \epsilon_{I3} \\
s^2 &= \frac{(2c_1 + c_1^2 - c_3^2)}{2\,(c_1 - c_4)\,(1 + c_1 + c_3)} \to \frac{c_1}{c_1 - c_4}
\end{aligned} \tag{6.27}$$

And finally, a trace (spin 0) mode:

$$\begin{aligned} \epsilon_{11} &= \epsilon_{22} = \frac{c_1+c_2+c_3}{2\left(1-c_2\right)}\epsilon_{33} = \left(c_1-c_4\right)s\epsilon_{03} \\ s^2 &= \frac{\frac{2}{c_1-c_4}+1}{\left(1+c_1+c_3\right)\left(\frac{2(1-c_2)}{c_1+c_2+c_3}-1\right)} \rightarrow \frac{c_1+c_2+c_3}{c_1-c_4} \end{aligned} \tag{6.28}$$

Comparing with the modes found in [40], the aether there replaces the polarization components ϵ_{0i} here, but otherwise the polarizations and speeds match.

6.3 Constraints on the aether Lagrangian parameters

Looking at the wave modes[3], we can put bounds on the aether parameters by requiring stability, positive energy, causality and the absence of ghosts [35]. First, we want positive squared speeds to avoid exponentially growing modes. In the limit of small parameters (always assumed in the following), this means

$$\frac{c_1}{c_1+c_4} \geq 0, \quad \frac{c_1+c_2+c_3}{c_1+c_4} \geq 0 \tag{6.29}$$

Requiring that the waves have positive energy yields [41]

$$c_1 > 0, \quad c_1+c_4 > 0 \tag{6.30}$$

This last condition also ensures that the aether modes aren't "ghost-like" [36]. Finally, the question of causality leads us to consider whether or not superluminal speeds should be rejected. This would imply

$$\frac{c_1}{c_1+c_4} \leq 1, \quad \frac{c_1+c_2+c_3}{c_1+c_4} \leq 1, \quad c_1+c_3 \leq 0 \tag{6.31}$$

[3]We remind the reader that the constraints in this section come from works which use a different metric signature. They cannot be directly compared with the speeds obtained in the previous section because of sign differences.

In the presence of small Lorentz violation, we would see only slightly superluminal speeds in some frames and physics would be local and causal [34]. With a dynamic aether however, some configurations can lead to energy-momentum flowing around closed curves [42]. Still, the formation of closed timelike curves is possible even in general relativity so this is not a firm objection to superluminal speeds.

The parameters are also constrained by observations. Cosmological considerations [43] give bounds of order 10^{-1}. Parameterized post-Newtonian parameters would suggest a bound of order 10^{-7} for the generic case [44] but if the parameters satisfy

$$c_2 = \frac{c_3^2 - c_1 c_3 - 2c_1^2}{3c_1}, \quad c_4 = -\frac{c_3^2}{c_1} \tag{6.32}$$

then all PPN parameters are the same as in general relativity [45] and the aether modes are superluminal. In the case of subluminal propagation, a study of the possible emission of metric-aether Čerenkov radiation by high energy cosmic rays [36] gives a constraint $|c_i| < 10^{-15}$, except in the special case

$$c_4 = 0, \quad c_1 + c_3 = 0, \quad c_2 = \frac{c_1}{1 - 2c_1} \tag{6.33}$$

where all the modes propagate exactly at the speed of light.

6.4 Other developments

Energy in this theory has been investigated using Einstein and Weinberg pseudotensors [41] and the Noether charge method [46]. Although the linearized modes have positive energy when the parameters satisfy the conditions previously mentioned, the question of positivity of energy in the full nonlinear theory remains unresolved. The total energy in an asymptotically flat spacetime is found to be

$$E = \frac{r_0}{2G}\left(1 - \frac{c_1 + c_4}{2}\right) \tag{6.34}$$

Compared to the value obtained in general relativity, $\frac{r_0}{2G_N}$, we see that the aether effectively renormalizes Newton's constant:

$$G_N = G\left[1 - \tfrac{1}{2}\left(c_1 + c_4\right)\right]^{-1} \tag{6.35}$$

This is confirmed by studying the Newtonian limit of the theory [43]. Note however that in a cosmological setting the effective Newton's constant receives a different correction which reduces the expansion rate of the Universe.

Finally, it is worth mentioning the recent study of time-independent spherically symmetric solutions [47, 48]. A three parameter family of vacuum solutions was found. Adding asymptotic flatness removes one parameter. Pure aether stars do not exist, but solutions are found for regular asymptotically flat perfect fluid stars and black holes.

7. Waves from a cusp in Einstein-aether theory

The procedure to find the gravitational waves emitted by the source here is more involved than in general relativity (section 3). There, each component of the metric perturbation had a separate source and all shared the same Green's function, so we only had to solve equation (3.15) once. Here, we have a system of 9 equations that mixes 9 components of h (remembering that $h_{00} = 0$ by our gauge choice and the equation for $\mathcal{G}_{03}$ is redundant):

$$\mathcal{G}_{\mu\nu}(h) = 8\pi G T_{\mu\nu} \tag{7.1}$$

To simplify the system, we go to Fourier space and we again pick the direction $k = (k_0, 0, 0, k_3)$, obtaining a system equivalent to (6.25) but without assuming a plane wave solution.

$$\begin{aligned}
2\mathcal{G}_{12} &= \left[k_3^2 - (1 + c_1 + c_3)\, k_0^2\right] h_{12} \qquad (7.2)\\
2\left(\mathcal{G}_{11} - \mathcal{G}_{22}\right) &= \left[k_3^2 - (1 + c_1 + c_3)\, k_0^2\right] (h_{11} - h_{22})\\
2\mathcal{G}_{I3} &= k_3 k_0 h_{0I} - (1 + c_1 + c_3)\, h_{I3} k_0^2\\
4\mathcal{G}_{0I} &= \left[(2 + c_1 - c_3)\, k_3^2 - 2(c_1 - c_4)\, k_0^2\right] h_{0I} - (2 + c_1 + c_3)\, k_3 k_0 h_{I3}\\
2\mathcal{G}_{II} &= -\left[(c_1 + 2c_2 + c_3 - 1)\, k_0^2 + k_3^2\right] h_{II} + 2(1 - c_2)\, k_0^2 h_{33} - 4 k_3 k_0 h_{03}\\
2\mathcal{G}_{33} &= (1 - c_2)\, k_0^2 h_{II} - (c_1 + c_2 + c_3)\, k_0^2 h_{33}\\
2\mathcal{G}_{00} &= k_3^2 h_{II} - 2(c_1 - c_4)\, k_3 k_0 h_{03}
\end{aligned}$$

We then have to treat each mode separately.

The components for the spin 2 modes appear in 1 equation each and are ready to be solved as before.

$$\begin{aligned} 16\pi G T_{12} &= \left[k_3^2 - (1 + c_1 + c_3)\, k_0^2\right] h_{12} \\ 16\pi G\,(T_{11} - T_{22}) &= \left[k_3^2 - (1 + c_1 + c_3)\, k_0^2\right] (h_{11} - h_{22}) \end{aligned} \tag{7.3}$$

From these, we can read the appropriate Green's function.

$$H\,(k) = 2\left[k_3^2 - (1 + c_1 + c_3)\, k_0^2\right]^{-1} \tag{7.4}$$

We will treat them in detail after looking at the other modes.

On the other hand, the components for the spin 1 modes have 2 equations each (the third and fourth lines in (7.2)). However, a combination of these 2 equations vanishes by conservation of T and allows us to relate the two components of that mode:

$$\begin{aligned} 0 &= 4\,(\mathcal{G}_{I3} k_3 - \mathcal{G}_{0I} k_0) \\ h_{I3} &= \frac{2\,(c_1 - c_4)\, s - (c_1 - c_3)\, s^{-1}}{c_1 + c_3} h_{0I} \end{aligned} \tag{7.5}$$

where $s \equiv \frac{k_0}{k_3}$ as before. Substituting h_{I3} in one of the original equations we find

$$16\pi G T_{0I} = \left[k_3^2 + \left(1 + \frac{1}{c_1 + c_3}\right)\left[(c_1 - c_3)\, k_3^2 - 2\,(c_1 - c_4)\, k_0^2\right]\right] h_{0I} \tag{7.6}$$

which gives us the Green's function for that mode.

Finally, there remains 3 equations for the spin 0 mode. However, there is only one combination that vanishes,

$$\begin{aligned} 0 &= 2\left(\mathcal{G}_{33} k_3^2 - \mathcal{G}_{00} k_0^2\right) \\ h_{03} &= \frac{1}{2\,(c_1 - c_4)\, s}\left[c_2 h_{II} + (c_1 + c_2 + c_3)\, h_{33}\right] \end{aligned} \tag{7.7}$$

apparently leaving 2 degrees of freedom.

$$\begin{aligned} 16\pi G T_{33} &= (1-c_2)\,k_0^2 h_{II} - (c_1+c_2+c_3)\,k_0^2 h_{33} \\ 16\pi G T_{II} &= -\left[(c_1+2c_2+c_3-1)\,k_0^2 + \left(1+\frac{2c_2}{(c_1-c_4)}\right)k_3^2\right] h_{II} \\ &\quad +2\left[(1-c_2)\,k_0^2 - \frac{(c_1+c_2+c_3)}{(c_1-c_4)}k_3^2\right] h_{33} \end{aligned} \tag{7.8}$$

This is due to the remaining gauge freedom, and fixing it should remove one of them. We won't treat the spin 0 and spin 1 modes further.

Going back to the spin 2 mode, we now need to take the inverse Fourier transform of the Green's function. To do so, we substitute back $\boldsymbol{k}$ instead of k_3. This is justified because $\mathcal{G}_{\mu\nu}$ has rotational symmetry and picking a direction helped us find a simple expression. That being said, our results are still only valid on the x_3 axis so the axes have to be oriented accordingly. Proceeding as in section 3, we find

$$\begin{aligned} H(x) &= 2\int \frac{d^3k}{(2\pi)^4}\, e^{i\boldsymbol{k}\cdot\boldsymbol{x}} \int_{-\infty}^{\infty} d\omega\, \frac{e^{-i\omega t}}{\boldsymbol{k}^2 - (1+c_1+c_3)\,\omega^2} \\ &= \frac{\theta(t)}{2\pi\,|\boldsymbol{x}|}\delta\left(\frac{t}{\sqrt{1+c_1+c_3}} - |\boldsymbol{x}|\right) \end{aligned} \tag{7.9}$$

As expected the delta function enforces the altered wave speed s we found in (6.26).

$$\begin{aligned} h_{12}(x) &= 4G\int d^4y\, \frac{1}{s\,|\boldsymbol{x}-\boldsymbol{y}|}\delta\left(x_0 - y_0 - |\boldsymbol{x}-\boldsymbol{y}|\,s^{-1}\right) T_{12}(y) \\ &= \frac{4G}{s}\int d^3y\, \frac{T_{12}\left(x_0 - |\boldsymbol{x}-\boldsymbol{y}|\,s^{-1}, \boldsymbol{y}\right)}{|\boldsymbol{x}-\boldsymbol{y}|} \\ &= \frac{4G}{s}\int \frac{d\omega}{2\pi}\int d^3y\, e^{-i\omega\left(x_0 - |\boldsymbol{x}-\boldsymbol{y}|s^{-1}\right)}\frac{T_{12}(\omega,\boldsymbol{y})}{|\boldsymbol{x}-\boldsymbol{y}|} \end{aligned} \tag{7.10}$$

To account for the wave speed, we redefine the retarded time and wave-vector in the direction of the observer.

$$\begin{aligned} t_R &= t - \frac{r}{s} \\ k_{\boldsymbol{x}} &= \omega\left(1, \frac{\boldsymbol{x}}{r}s^{-1}\right) \end{aligned} \tag{7.11}$$

Thus we find a very similar expression to (3.26) for the wave.

$$\begin{aligned} h_{12}(x) &= \frac{2G}{\pi s}\int d\omega\,\frac{e^{-i\omega t_R}}{r}\int d^3\boldsymbol{y}\,e^{-i\boldsymbol{k_x}\cdot\boldsymbol{y}}T_{12}(\omega,\boldsymbol{y}) \\ &= \frac{2G}{\pi r s}\int d\omega\,e^{-i\omega t_R}T_{12}(k_{\boldsymbol{x}}) \end{aligned} \tag{7.12}$$

At first sight, it might seem that the only differences are a slight change in amplitude (due to the factor s^{-1}) and a later time of arrival, but as we will see, the small change in the wave vector $k_{\boldsymbol{x}}$ will also change how the source points are distributed according to retarded time, with significant effects on the wave profile.

7.1 Spectrum

Because of the different wave vector, we need to revise our expression for the string energy-momentum tensor (2.34). After we use the cusp Taylor expansion in the integrals

$$I^{\mu}_{\pm} \approx \int_{-1}^{1} d\sigma_{\pm}\,\left(\dot{X}^{\mu}_{\pm 0}+\ddot{X}^{\mu}_{\pm 0}\sigma_{\pm}\right)\,e^{-\frac{i}{2}k\cdot X_{\pm}} \tag{7.13}$$

we find an extra term in the phase compared to (4.3):

$$\begin{aligned} k_{\boldsymbol{x}}\cdot X_{\pm} &= \left(1,s^{-1}\dot{\mathbf{X}}_0\right)\cdot\left(\dot{X}_{\pm 0}\sigma_{\pm}+\frac{1}{2}\ddot{X}_{\pm 0}\sigma_{\pm}^2+\frac{1}{6}\dddot{X}_{\pm 0}\sigma_{\pm}^3\right) \\ &= \left(s^{-1}-1\right)\sigma_{\pm}-\frac{1}{6}s^{-1}\ddot{X}_{\pm}^2\sigma_{\pm}^3 \end{aligned} \tag{7.14}$$

Since we only need T_{12}, the term with $\dot{X}^{\mu}_{\pm 0}$ doesn't contribute. Also, with the proper rotation (as explained below (4.11)), we find $\ddot{X}^{(1}_{+0}\ddot{X}^{2)}_{-0}=\frac{1}{2}\left|\ddot{X}_{+0}\right|\left|\ddot{X}_{-0}\right|$. Then if we generalize our normalized variables (4.15) by including appropriate speed factors,

$$\begin{aligned} \tilde{h}(\tilde{\omega},\boldsymbol{x}) &\equiv \frac{rs}{G\mu\left|\ddot{X}_{+0}\right|\left|\ddot{X}_{-0}\right|}h^{12}(\omega,\boldsymbol{x}) \\ \tilde{\omega} &\equiv \frac{\left|\ddot{X}_{+0}\right|\left|\ddot{X}_{-0}\right|}{12s}\omega \end{aligned} \tag{7.15}$$

the wave spectrum is found to be

$$\begin{aligned} \tilde{h}\left(\tilde{\omega}, \boldsymbol{x}\right) &= \tilde{\omega}^{-\frac{4}{3}} K\left(a\tilde{\omega}\right) K\left(a^{-1}\tilde{\omega}\right) \\ K\left(w\right) &= \int_{-w^{\frac{1}{3}}}^{w^{\frac{1}{3}}} du\, u\, e^{-iw^{\frac{2}{3}}\frac{c}{a}u} e^{iu^3} \end{aligned} \tag{7.16}$$

where we introduced a new speed parameter[4],

$$c \equiv \frac{6\left(1-s\right)}{\left|\ddot{X}_{+0}\right|\left|\ddot{X}_{-0}\right|} \tag{7.17}$$

Note that c will be positive for subluminal speeds and negative for superluminal speeds.

We did not find an expression in terms of known functions for the integral K. We used numerical integration to plot the spectrum for various values of c (figure 7.1). For any non-zero value of c, we find that the spectrum has points where the amplitude is zero. We plotted the absolute value of the spectrum, but it is purely real as it was in the general relativity case, so these points correspond to phase inversions (the phase changes by π). For positive values of c, we also see that the spectrum is much less regular and can have a much greater amplitude at higher frequencies. For negative values of c on the other hand, the opposite is true and the power seems to be limited to low frequencies. These features will be easier to understand by looking at the wave profiles.

7.2 Wave profile

Again, to be consistent with the normalized frequency, we generalize the normalized retarded time by adding a factor of s.

$$\tilde{t}_R = \frac{12 s t_R}{\left|\ddot{X}_{+0}\right|\left|\ddot{X}_{-0}\right|} \tag{7.18}$$

[4]The choice of the symbol c seemed appropriate at the time, since it includes the aether Lagrangian parameters c_i. It should not be confused with the speed of light.

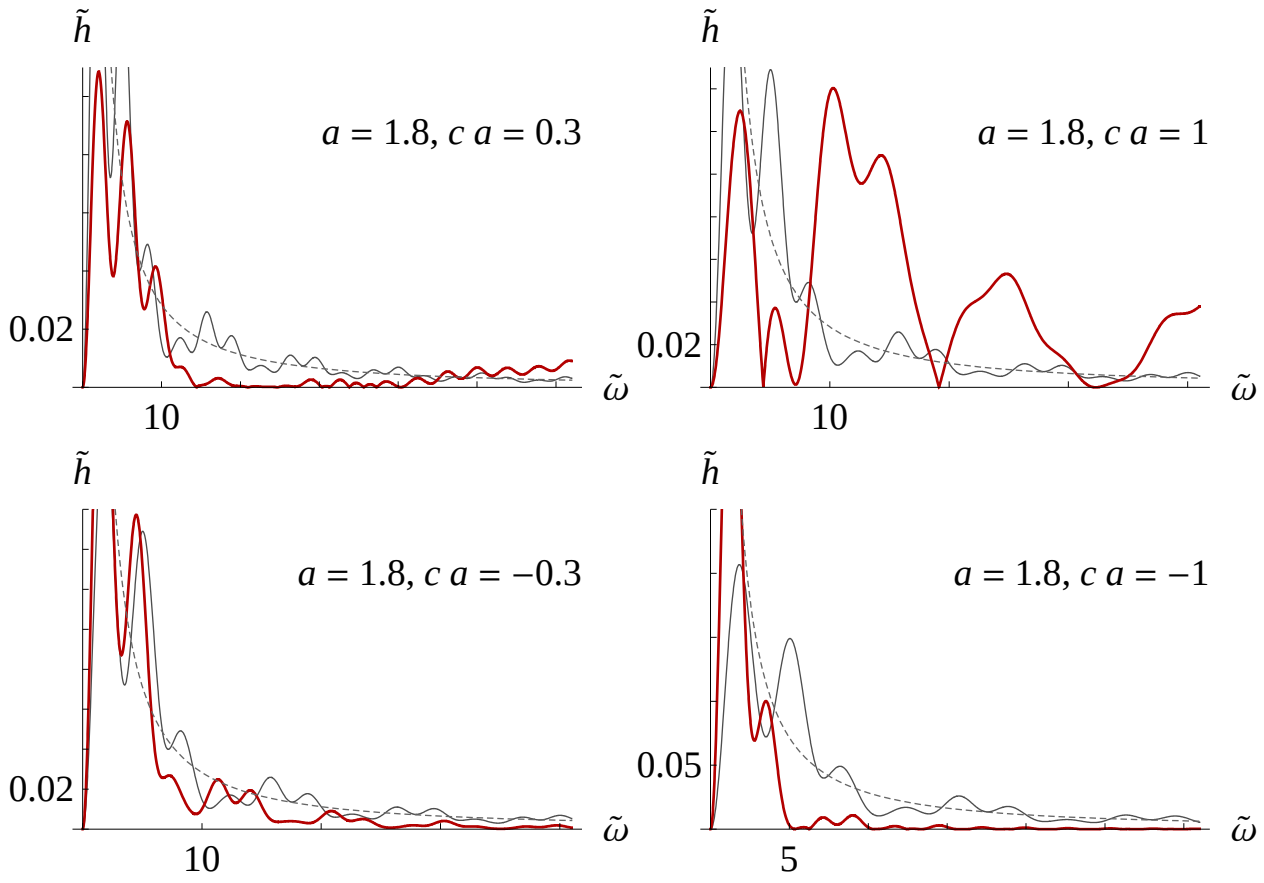

Figure 7.1: Gravitational wave spectra from a string cusp in Einstein-aether theory for both subluminal ($c > 0$) and superluminal ($c < 0$) waves. c is a parameter combining wave speed, cusp acceleration and cusp length.

Note that $\tilde{h}\left(\tilde{t}_R\right)$ requires no speed factor and remains as before (4.19), i.e.

$$\tilde{h}\left(\tilde{t}_R\right) = \frac{r}{12G\mu} h\left(t_R, \boldsymbol{x}\right) \tag{7.19}$$

A survey of wave profiles for various values of the 2 parameters a and c reveals a diversity of shapes, but as was the case before, many features are artefacts of the edges of the source patch. We first observe (figure 7.2) that for negative values of c the waves tend to smooth out, which is consistent with the spectrum having high frequencies suppressed. On the other

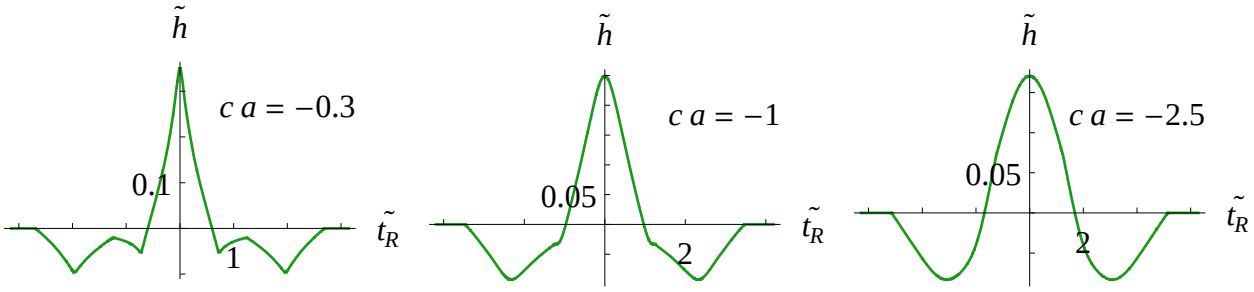

Figure 7.2: Profile of superluminal gravitational waves emitted by a string cusp in Einstein-aether theory, for various values of our speed parameter c, with the ratio of the $+$ and $-$ cusp acceleration amplitudes $a = 1.8$.

hand, figure 7.3 shows that positive values of c introduce extra structure at the center of the wave which tends to widen and eventually smooth out for larger values of c. Two notable features of this structure are first, a discontinuity and second, a doubling of the central peak when $a \neq 1$. The discontinuity and sharpness of the peaks are consistent with the spectrum having a relatively large amplitude at high frequencies.

To verify if these features are physical, and to better understand them, we again look at how the source is distributed in terms of retarded time. We will look at the cases $a = 1.8$ with $c = \pm 1$ and the case $a = c = 1$. First, figure 7.4 shows the wave and source for a

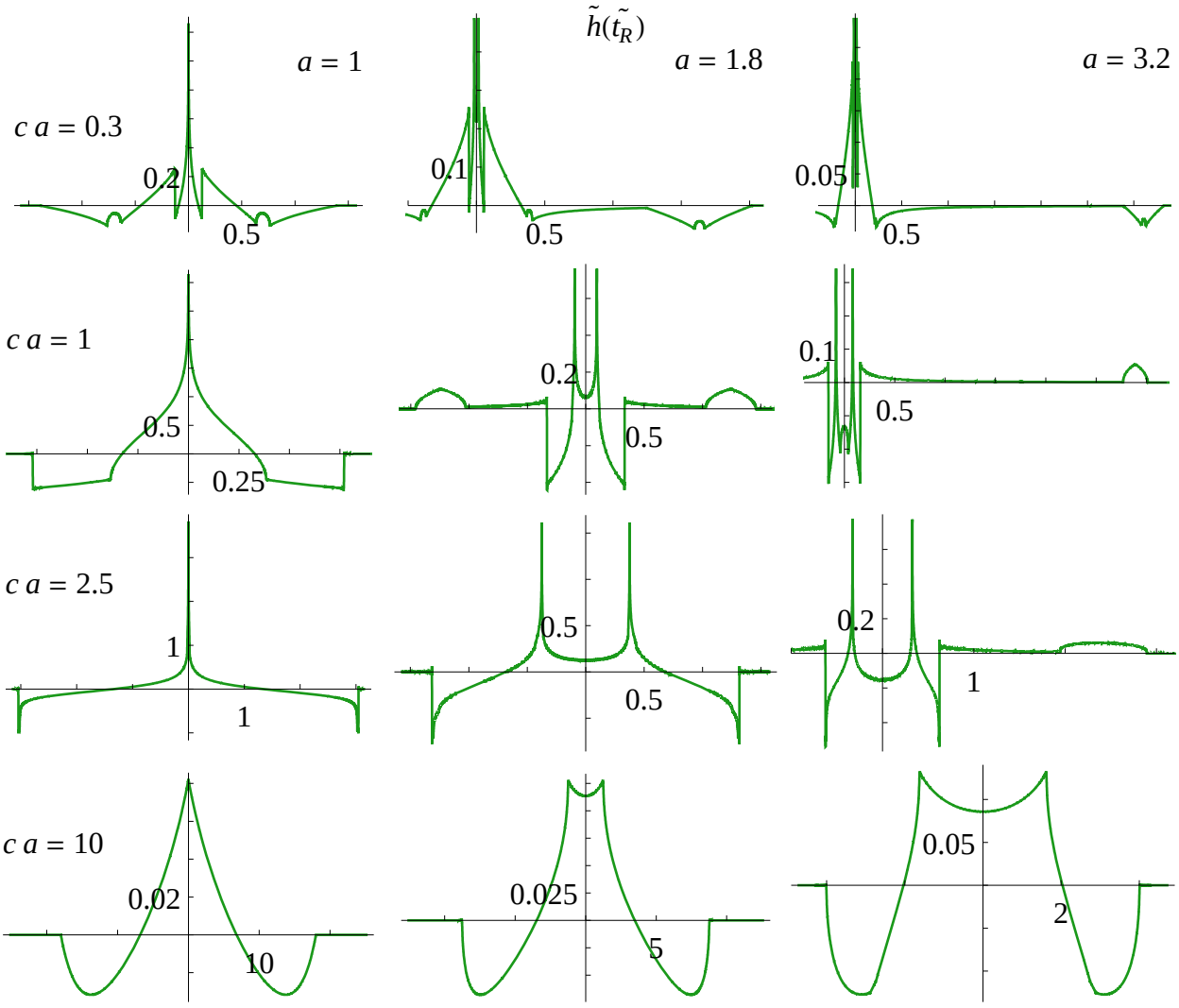

Figure 7.3: Profile of subluminal gravitational waves emitted by a string cusp in Einstein-aether theory, for various values of our speed parameter c and of a, the ratio of the $+$ and $-$ cusp acceleration amplitudes.

superluminal wave. The distribution of the source is not much different than our general relativity reference ($c = 0$, figure 4.4), but there seems to be less distortion at the origin. The smoothing of the peak is not hard to understand. Since the cusp tip no longer reaches the wave speed, there is less "piling up" of energy.

There is more to say about the subluminal cases. First, let's observe the case $a \neq 1$ (figure 7.5). We chose $c = 1$ because the extra structure of the peak is wide enough to be clearly seen and it has not started to smooth out. The doubling of the peak can be understood intuitively if we think of the source as a single point that accelerates up to the speed of light and slows down afterwards. Just like a plane reaching the speed of sound encounters the sound barrier, when the source reaches the speed of the wave energy accumulates. For speeds lower than the speed of light, this will occur twice. Of course, the situation is more complicated since only quadrupolar motion transverse to the direction of observation produces gravitational waves, but with the appropriate transverse motion, the analogy applies. In the figure of the worldsheet patch, we drew a line at points where the string moves at the speed of the wave. We can see that this line crosses 2 saddle points and these correspond to the two peaks. Looking at the 3d worldsheet, we see that at the moment of the cusp (see figure 2.3 to recall it's location) the points that contribute to the peaks are slightly below the tip, where the string speed is very close to the wave speed. A closer examination would be required to verify that the longitudinal component (in the direction of the observer) of the string speed matches the wave speed.

The other feature we observed is the discontinuity on each side of the double peak. Again looking at the worldsheet, starting from the left, we observe a single source line for each time, but at the time of the discontinuity, an extra point appears, which expands in a loop later. Furthermore, this extra point seems to be very close to the gray line (but not exactly on it), meaning that the string at that point moves with a longitudinal speed equal to the speed of the wave. So we can conclude that both the double peak and the discontinuities

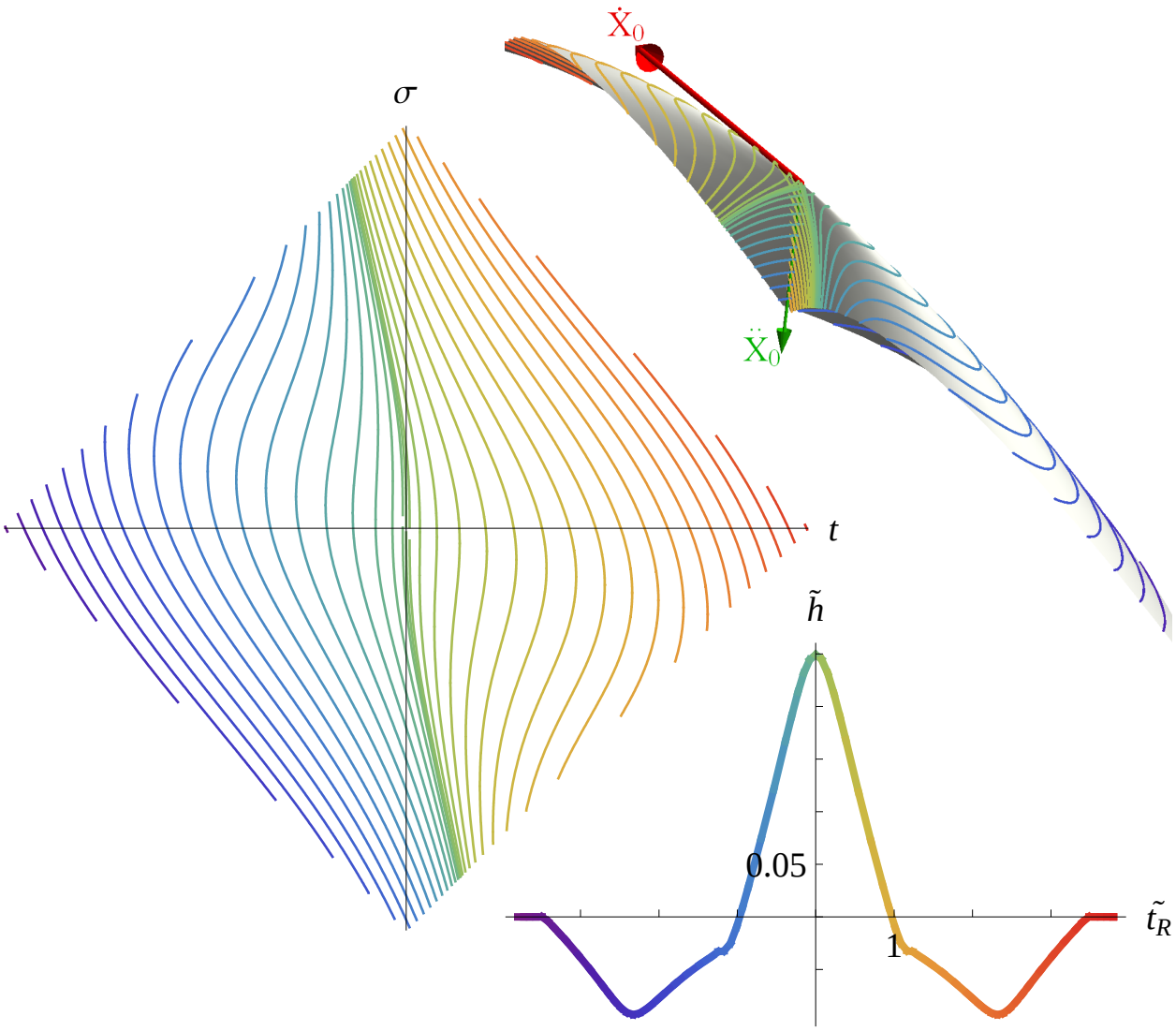

Figure 7.4: Comparison of the wave profile and its source, with $a = 1.8$, $ca = -1$. Each color corresponds to a specific retarded time, allowing us to locate the region of the source on the worldsheet (in space: upper right, or in worldsheet coordinates: left) that produces a point of the wave (lower right).

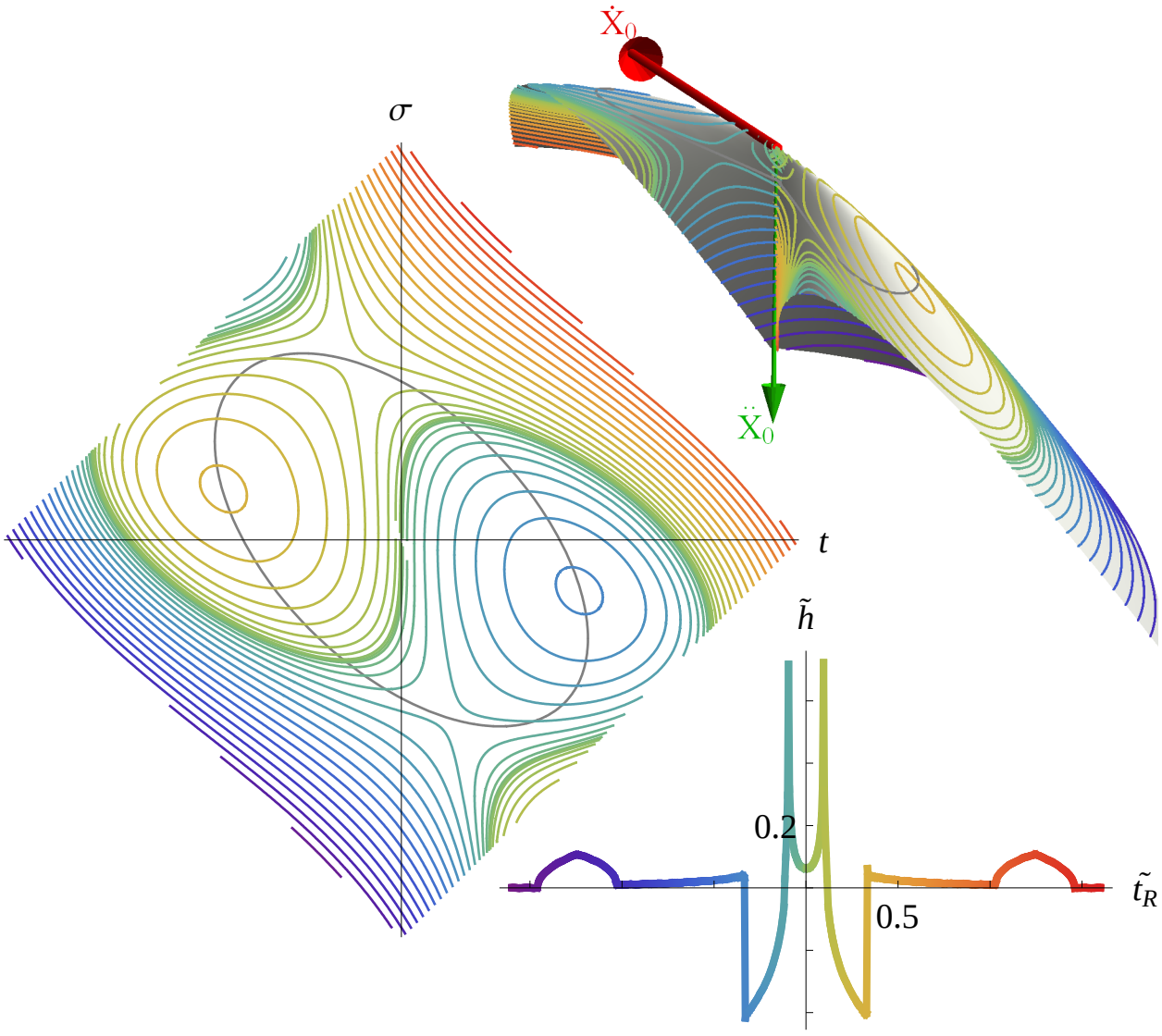

Figure 7.5: Comparison of the wave profile and its source, with $a = 1.8$, $ca = 1$.

are real effects, in the sense that they are not due to the edges of the worldsheet or our approximations. Of course, we would expect them to be smoother and possibly modified in some other way in more realistic models, for example for strings with a non-zero width.

We can also understand by looking at this figure why the extra wave structure tends to widen and eventually smooth out for larger values of the speed parameter. There are 2 ways in which c can become larger. Either decrease the speed or the acceleration at the cusp. In both cases, this has the effect of stretching the source line pattern which is easily understood by thinking only of the gray line where string and wave speeds are equal. Obviously, lowering the wave speed will stretch this loop, but similarly, lowering the cusp acceleration will mean a larger area around it will have a speed higher than the wave's. Since our patch has finite size, as the pattern stretches, more and more of it will be cut off, eventually loosing the first appearance of the second source line (smoothing out the discontinuity) and also the saddle points (reducing the sharpness of the double peak).

The last case we will observe is $a = c = 1$ (figure 7.6). In this case, the extra symmetry of the worldsheet results in both saddle points contributing to the same retarded time, namely $t_R = 0$. The entire string at the moment of the cusp also contributes to $t_R = 0$, the cusp in this case being a single straight line along $\ddot{\mathbf{X}}_0$. Thus there is a single peak in this case. The discontinuity is also visible here.

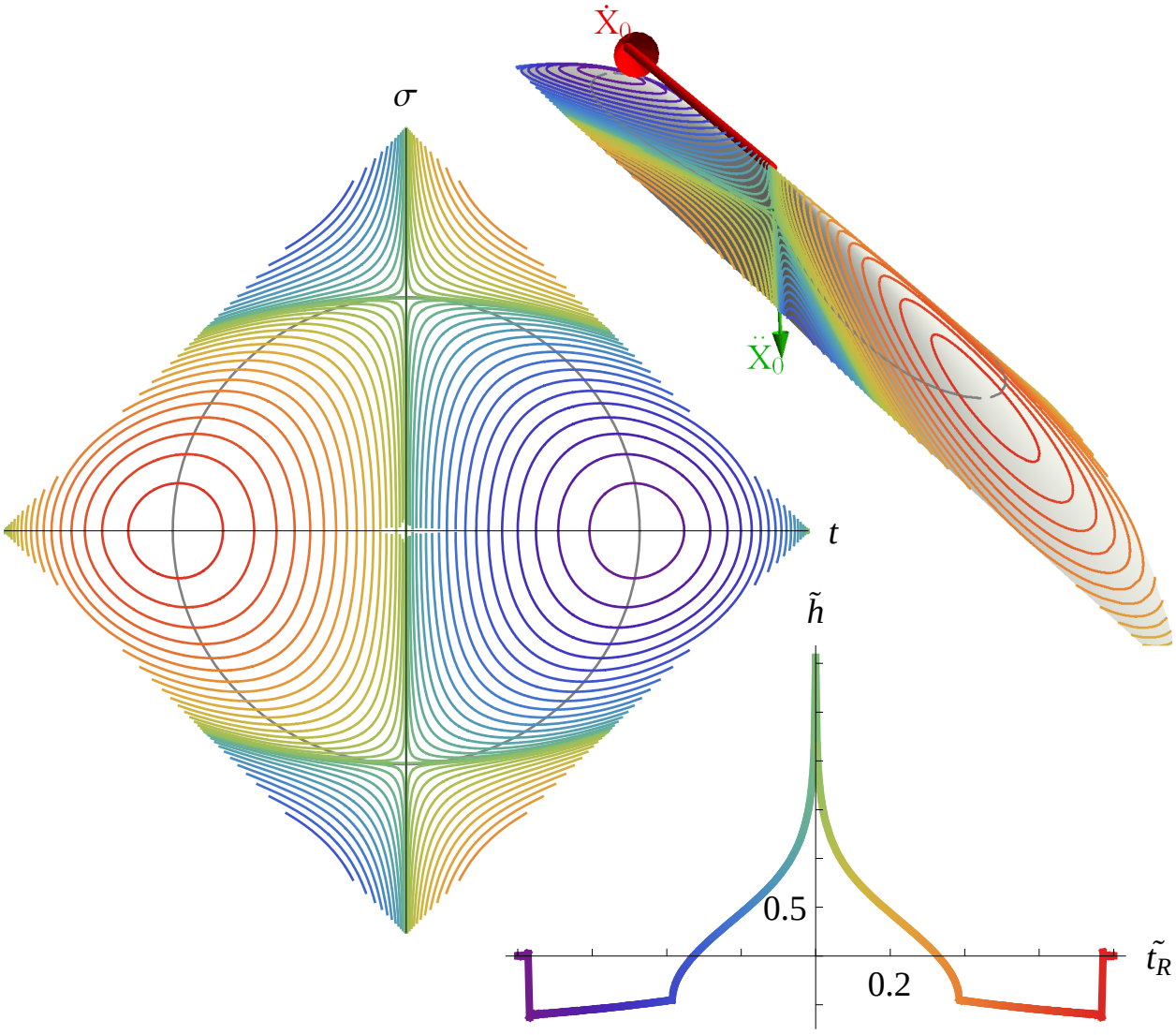

Figure 7.6: Comparison of the wave profile and its source, with $a = c = 1$.

8. Conclusion

We studied the gravitational waves emitted by a string cusp in the context of Einstein-aether theory. The dynamic timelike aether field picks a preferred frame at each point in spacetime, thus spontaneously breaking Lorentz symmetry. This gives rise in the linearized theory to five wave modes. We found the spectrum and wave profile of the usual transverse traceless mode for waves produced by an idealized string cusp. The string is taken to have zero width and represented by a Taylor expansion around the cusp, whose tip moves at the speed of light in the direction of the observer. The source is a square patch of the string worldsheet in null worldsheet coordinates. The spectrum contained integrals that had to be computed numerically and the wave profile was obtained by sampling the spectrum and performing a discrete Fourier transform. The results were plotted and analyzed for various values of two free parameters: the ratio a of the norm of the $+$ and $-$ (left and right movers) string acceleration components at the cusp ($\left|\ddot{X}_{\pm 0}\right|$) and a speed parameter c that depends on these acceleration components (in units of the string length l) and the wave speed s. We found distinctive features compared to the waves obtained in pure general relativity.

All the observed differences between the waves with and without the aether field stem from the modified wave speed $s = \frac{1}{\sqrt{1+c_1+c_2}}$. It can be both lower or higher than the speed of light, although the former is much more constrained by observations than the latter. If the wave is superluminal, then no point of the string, in particular the cusp, reaches this speed and the gravitational wave burst is not as intense. The power is concentrated in lower frequencies and the profile is smoother than without the aether. If the wave is subluminal, the opposite is true. There is more power at high frequencies and some extra structure

appears in the wave profile. If $a \neq 1$, the central peak splits in two and in all cases, a discontinuity appears on both sides of the peak. Other non-physical features were observed to be the result of the edges of the source patch.

For cosmic strings with high enough tensions, gravitational wave bursts from cusps could be detected by the gravitational wave detectors LISA and Advanced LIGO planned for operation in 2015 and 2013 respectively. It remains to be seen if the distinctive features of the waves in Einstein-aether theory could be observed. To do so, we need to examine the amplitude of the spectrum at the frequencies the detectors are sensitive to. This may be difficult since the main parameter that determines the strength of the aether effects c depends not only on the aether Lagrangian parameters c_i which are somewhat constrained, but also on the cusp acceleration amplitudes $\left|\ddot{X}_{+0}\right| \left|\ddot{X}_{-0}\right|$. We need more specific models to determine possible values for these. If we assume that they are of order 1, then c would be small and we would need relatively high frequencies to observe the Lorentz violating effects.

One could also look at the other modes that are not usually present without Lorentz violation. These could also provide a detectable signature of Lorentz violation. The spin 1 mode has a similar Green's function (7.6) and the analysis should not be much more complicated than it was for the spin 2 mode. For the spin 0 mode however, we need to specify further gauge constraints to remove one of the apparent two degrees of freedom in the remaining system (7.8) and the only freedom left is rigid (constant in time) coordinate transformations. Once this is realized, it is probable that the analysis would be similar to the other two modes.

This work could be complimented by studying other aspects of the waves or more realistic models for the strings. Firstly, given that the wave burst is an event of short duration we should be concerned that the probability of being in the right direction at the right time might be very small. We could study the waves at small angles from the cusp speed direction,

as was previously done in general relativity [21] to see if the aether signature is still present. We should also consider the effects of the cosmic string width. Obviously, our zero-width approximation would break down at points where the string radius of curvature becomes comparable to the string width, namely at the cusp. Cosmic superstrings do not require this assumption, but for D-strings, there are other effects to consider. For example near the tip of the cusp, fundamental strings attached to the D-string can stretch between the two branches of the cusp, providing extra tension which probably prevents the tip from forming. Finally the self gravity of the string at the cusp might be significant. These possible causes of "smoothing" might significantly reduce not only the wave burst intensity, but also the distinctive wave features in Einstein-aether theory.

Bibliography

[1] T. Jacobson, S. Liberati, and D. Mattingly, "Quantum gravity phenomenology and Lorentz violation," *Springer Proc. Phys.* **98** (2005) 83–98, `gr-qc/0404067`. Also in: Particle Physics and the Universe (Dubrovnik 2003).

[2] T. W. B. Kibble, "Cosmic strings reborn?," `astro-ph/0410073`.

[3] A. Vilenkin, "Cosmic strings: progress and problems," in *Inflating Horizons of Particle Astrophysics and Cosmology*, H. Suzuki, J. Yokoyama, Y. Suto, and K. Sato, eds. Universal Academy Press, Tokyo, 2006. `hep-th/0508135`.

[4] M. Sakellariadou, "Cosmic strings," *Lect. Notes Phys.* **718** (2007) 247–288, `hep-th/0602276`. Also in: Quantum simulations via analogues (Dresden 2005).

[5] A. Vilenkin and E. P. S. Shellard, *Cosmic Strings and Other Topological Defects*. Cambridge University Press, 1994.

[6] M. R. Anderson, *The Mathematical Theory of Cosmic Strings, Cosmic Strings in the Wire Approximation*. Series in High Energy Physics, Cosmology and Gravitation. Institute of Physics Publishing, Bristol, 2003.

[7] M. B. Hindmarsh and T. W. B. Kibble, "Cosmic strings," *Rept. Prog. Phys.* **58** (1995) 477–562, `hep-ph/9411342`.

[8] R. Jeannerot, J. Rocher, and M. Sakellariadou, "How generic is cosmic string formation in SUSY GUTs," *Phys. Rev. D* **68** (2003) 103514, `hep-ph/0308134`.

[9] E. Jeong and G. F. Smoot, "Search for cosmic strings in CMB anisotropies," *Astrophys. J.* **624** (2005) 21–27, astro-ph/0406432.

[10] E. Jeong and G. F. Smoot, "The Validity of the Cosmic String Pattern Search with the Cosmic Microwave Background," *Astrophys. J. Lett.* **661** (2007) L1, astro-ph/0612706.

[11] N. Bevis, M. Hindmarsh, M. Kunz, and J. Urrestilla, "Fitting CMB data with cosmic strings and inflation," astro-ph/0702223.

[12] N. Kaiser and A. Stebbins, "Microwave anisotropy due to cosmic strings," *Nature* **310** (1984) 391–393.

[13] M. V. Sazhin, M. Capaccioli, G. Longo, M. Paolillo, and O. S. Khovanskaya, "The true nature of CSL-1." Submitted to Mon. Not. Roy. Astron. Soc., 2006.

[14] R. E. Schild, I. S. Masnyak, B. I. Hnatyk, and V. I. Zhdanov, "Anomalous fluctuations in observations of Q0957+561 A,B: Smoking gun of a cosmic string?," *Astron. Astrophys.* **422** (2004) 477–482, astro-ph/0406434.

[15] K. J. Mack, D. H. Wesley, and L. J. King, "Observing cosmic string loops with gravitational lensing surveys," astro-ph/0702648. Submitted to Phys. Rev. D.

[16] F. A. Jenet *et al.*, "Upper bounds on the low-frequency stochastic gravitational wave background from pulsar timing observations: Current limits and future prospects," *Astrophys. J.* **653** (2006) 1571–1576, astro-ph/0609013.

[17] V. Berezinsky, B. Hnatyk, and A. Vilenkin, "Gamma ray bursts from superconducting cosmic strings," *Phys. Rev. D* **64** (2001) 043004, astro-ph/0102366.

[18] J. Polchinski, "Introduction to cosmic F- and D-strings," in *String theory: From gauge interactions to cosmology*, L. Baulieu, J. de Boer, B. Pioline, and E. Rabinovici, eds. Springer, Cargèse, 2005. `hep-th/0412244`.

[19] J. Preskill and A. Vilenkin, "Decay of metastable topological defects," *Phys. Rev. D* **47** (1993) 2324–2342, `hep-ph/9209210`.

[20] C. W. Misner, K. S. Thorne, and J. A. Wheeler, *Gravitation*. W.H. Freeman, New York, 1973.

[21] T. Damour and A. Vilenkin, "Gravitational wave bursts from cusps and kinks on cosmic strings," *Phys. Rev. D* **64** (Aug, 2001) 064008, `gr-qc/0104026`.

[22] Wolfram Research, "Hypergeometric." `http://functions.wolfram.com/HypergeometricFunctions/`. Retrieved on 2007-10-06.

[23] Wolfram Research, "Incomplete gamma function." `http://functions.wolfram.com/GammaBetaErf/Gamma2/`. Retrieved on 2007-10-06.

[24] Wolfram Research, "Exponential integral E." `http://functions.wolfram.com/GammaBetaErf/ExpIntegralE/`. Retrieved on 2007-10-06.

[25] G. Amelino-Camelia, "The three perspectives on the quantum-gravity problem and their implications for the fate of Lorentz symmetry," in *Recent Developments in Theoretical and Experimental General Relativity, Gravitation and Relativistic Field Theories*, M. Novello, S. E. Perez Bergliaffa, and R. Ruffini, eds. World Scientific, Rio de Janeiro, 2005. `gr-qc/0309054`.

[26] V. A. Kostelecký and S. Samuel, "Spontaneous breaking of Lorentz symmetry in string theory," *Phys. Rev. D* **39** (Jan., 1989) 683–685.

[27] G. Chapline, E. Hohlfeld, R. B. Laughlin, and D. I. Santiago, "Quantum phase transitions and the breakdown of classical general relativity," *Int. J. Mod. Phys.* **A18** (2003) 3587–3590, gr-qc/0012094.

[28] G. Amelino-Camelia, "Doubly special relativity," *Nature* **418** (2002) 34–35, gr-qc/0207049.

[29] J. Kowalski-Glikman, "Introduction to doubly special relativity," *Lect. Notes Phys.* **669** (2005) 131–159, hep-th/0405273.

[30] J. M. Carmona and J. L. Cortes, "Departures from special relativity beyond effective field theories." Contribution to the Festschrift in honor of Adriano Di Giacomo's 70th birthday, 2006.

[31] D. Colladay and V. A. Kostelecky, "Lorentz-violating extension of the standard model," *Phys. Rev. D* **58** (1998) 116002, hep-ph/9809521.

[32] V. A. Kostelecky, "Gravity, Lorentz violation, and the standard model," *Phys. Rev.* **D69** (2004) 105009, hep-th/0312310.

[33] J. Collins, A. Perez, D. Sudarsky, L. Urrutia, and H. Vucetich, "Lorentz invariance: An additional fine-tuning problem," *Phys. Rev. Lett.* **93** (2004) 191301, gr-qc/0403053.

[34] D. Mattingly, "Modern tests of Lorentz invariance," *Living Rev. Rel.* **8** (2005) 5, gr-qc/0502097.

[35] C. Eling, T. Jacobson, and D. Mattingly, "Einstein-aether theory," in *Deserfest: A Celebration of the Life and Works of Stanley Deser*, J. Liu, M. J. Duff, K. S. Stelle, and R. P. Woodard, eds. World Scientific, Ann Arbor, 2006. gr-qc/0410001.

[36] J. W. Elliott, G. D. Moore, and H. Stoica, "Constraining the new aether: Gravitational Cherenkov radiation," *JHEP* **08** (2005) 066, hep-ph/0505211.

[37] P. Peldan, "Actions for gravity, with generalizations: A Review," *Class. Quant. Grav.* **11** (1994) 1087–1132, gr-qc/9305011.

[38] J. F. Barbero G. and E. J. S. Villasenor, "Lorentz Violations and Euclidean Signature Metrics," *Phys. Rev. C* **68** (2003) 087501, gr-qc/0307066.

[39] B. Z. Foster, "Metric redefinitions in Einstein-aether theory," *Phys. Rev. D* **72** (2005) 044017, gr-qc/0502066.

[40] T. Jacobson and D. Mattingly, "Einstein-aether waves," *Phys. Rev. D* **70** (2004) 024003, gr-qc/0402005.

[41] C. Eling, "Energy in the Einstein-aether theory," *Phys. Rev. D* **73** (2006) 084026, gr-qc/0507059.

[42] E. A. Lim, "Can we see Lorentz-violating vector fields in the CMB?," *Phys. Rev. D* **71** (2005) 063504, astro-ph/0407437.

[43] S. M. Carroll and E. A. Lim, "Lorentz-violating vector fields slow the universe down," *Phys. Rev. D* **70** (2004) 123525, hep-th/0407149.

[44] M. L. Graesser, A. Jenkins, and M. B. Wise, "Spontaneous Lorentz violation and the long-range gravitational preferred-frame effect," *Phys. Lett.* **B613** (2005) 5–10, hep-th/0501223.

[45] B. Z. Foster and T. Jacobson, "Post-Newtonian parameters and constraints on Einstein- aether theory," *Phys. Rev. D* **73** (2006) 064015, gr-qc/0509083.

[46] B. Z. Foster, "Noether charges and black hole mechanics in Einstein-aether theory," *Phys. Rev. D* **73** (2006) 024005, gr-qc/0509121.

[47] C. Eling and T. Jacobson, "Spherical Solutions in Einstein-Aether Theory: Static Aether and Stars," *Class. Quant. Grav.* **23** (2006) 5625–5642, gr-qc/0603058.

[48] C. Eling and T. Jacobson, "Black holes in Einstein-aether theory," *Class. Quant. Grav.* **23** (2006) 5643–5660, gr-qc/0604088.

[49] S. M. Carroll, *Spacetime and Geometry: An Introduction to General Relativity.* Addison Wesley, San Francisco, 2004.

A. Coordinate transformations and diffeomorphisms

Here, we review how infinitesimal coordinate transformations lead to the use of the Lie derivative [49, Appendices A and B] and we detail some aspects of the passive and active viewpoints that can be confusing. Let us first establish some notation. We will work with a manifold M and coordinates

$$\begin{aligned} x : M &\rightarrow \mathbb{R}^n \\ p &\mapsto x(p) \end{aligned} \tag{A.1}$$

More precisely, the coordinates are defined on a patch $U \subset M$, but we can neglect this in our discussion. We will often suppress indices, especially on the coordinates. $x(p)$ will always refer to a specific coordinate system, functions on M. On the other hand, when x is taken as an argument, as in $f(x)$, it should be thought of simply as values; the coordinate system they represent depends on the function. Finally, $[\cdots](x)$ means the expression in brackets is evaluated at x.

Consider an infinitesimal change of coordinates given by a vector field ξ and infinitesimal parameter t,

$$y^\mu(p) = x^\mu(p) + t\xi^\mu(p) \tag{A.2}$$

and the corresponding Jacobian matrix

$$J^\mu{}_\nu \equiv \frac{\partial y^\mu}{\partial x^\nu} = \delta^\mu{}_\nu + t\xi^\mu{}_{,\nu} \tag{A.3}$$

Then given a function $f(x)$, define a "transformed" function f' that takes the new coordinates as argument:

$$\begin{aligned} f'(y(p)) &\equiv f(x(p)) \\ f'(x) &= f(x - t\xi) \\ &\approx f(x) - t\xi^\mu \partial_\mu f(x) \\ &= f(x) - \mathcal{L}_{t\xi} f(x) \end{aligned} \tag{A.4}$$

Again, here f' takes x as new coordinates and f as old ones, so $f'(x)$ and $f(x)$ are at different points. Applying this formula to the original coordinates, we find an expression that merits a few comments:

$$x'(x) = x(x) - t\xi \tag{A.5}$$

First, according to how we defined f', $x'(x)$ represents the *old* coordinates as a function of the *new* ones, not the other way around. That is why we didn't call the new coordinates x' (as is often the case) but y, otherwise the notation is inconsistent: on all functions and other objects the prime means the argument is new coordinates, and x is the name of the old coordinates. Second, by definition $x(x)$ is just the identity function (as is $y(x)$) so on the right $x(x)$ just gives back the value of the *new* coordinates we plug in on the left. Things look less confusing if we write this as $x'(y) = y - t\xi$.

A vector field X transforms in two ways. Like functions, $X'(x) = X(x - t\xi)$, but also,

$$\begin{aligned} X(p) &= [X^\mu \partial_\mu](p) \\ &= \left[X^\nu J^\mu{}_\nu \frac{\partial}{\partial y^\mu}\right](p) \end{aligned} \tag{A.6}$$

Together, we find

$$\begin{aligned} \left[X'^\mu \frac{\partial}{\partial y^\mu}\right](x) &= \left[X^\nu J^\mu{}_\nu \frac{\partial}{\partial y^\mu}\right](x - t\xi) \\ &\approx \left[X^\nu \left(\delta^\mu{}_\nu + t\xi^\mu{}_{,\nu}\right) \frac{\partial}{\partial y^\mu}\right](x) - \left[t\xi^\nu X^\mu{}_{,\nu} \frac{\partial}{\partial y^\mu}\right](x) \end{aligned} \tag{A.7}$$

So to first order in t, the components satisfy

$$\begin{aligned} X'^{\mu}(x) &= \left[X^{\mu} + t\xi^{\mu}{}_{,\nu}X^{\nu} - t\xi^{\nu}X^{\mu}{}_{,\nu}\right](x) \\ &= X^{\mu}(x) - \mathcal{L}_{t\xi}X^{\mu}(x) \end{aligned} \tag{A.8}$$

Let's now turn to so-called active transformations. Given a manifold, we can define maps from M to other spaces (sections of various bundles over M) and think of the images of these maps as objects living on the manifold. For example, functions map M onto $(M\times)\,\mathbb{R}$ and vector fields map $M \to TM$ the tangent bundle. Then, given a diffeomorphism $\phi : M \to M$, we can take its composition with these maps and think of the resulting images as the transformed objects. To understand how the composition is realized on different objects, it is clearer if we take ϕ to be an invertible map to a different manifold $\phi : M \to N$. For example, we define the push-forward ϕ_* of a function as the "transformed" function on N.

$$\begin{aligned} f : M &\to \mathbb{R} \\ p &\mapsto f(p) \\ \phi_* f : N &\to \mathbb{R} \\ \phi p &\mapsto \phi_*\left[f(p)\right] \equiv (\phi_* f)(\phi p) = \left(f \circ \phi^{-1}\right)(\phi p) = f(p) \end{aligned} \tag{A.9}$$

We see that we must compose with ϕ^{-1} to get from N to M (and then to $\mathbb{R}$). We also define the pull-back ϕ^* as the inverse operation, i.e. given $g : N \to \mathbb{R}$, $\phi^* g = \phi_*^{-1} g$. Note that if ϕ is not invertible, which is never the case for a coordinate change, then only the pull-back would exist for functions and covectors, only the push-forward for vectors and neither for general tensors.

In practice we use functions of coordinates, which are themselves functions over M.

$$\begin{aligned} f : \mathbb{R}^n &\to \mathbb{R} \\ x &\mapsto f\left(x^{-1}(x)\right) \end{aligned} \tag{A.10}$$

It would seem natural to define the transformed function in terms of the new coordinates $\phi_* x$, but this would not correspond to our passive change of coordinates. Indeed, since $(\phi_* x)(\phi p) = x(p)$, we would find that the function doesn't change:

$$\begin{aligned} \phi_* f : \mathbb{R}^n &\rightarrow \mathbb{R} \\ (\phi_* x)(\phi p) &\mapsto (\phi_* f)((\phi_* x)(\phi p)) = f(x(p)) \\ x &\mapsto (\phi_* f)(x) = f(x) \end{aligned} \tag{A.11}$$

The last result applied to the coordinates themselves may again seem a bit odd $(\phi_* x)(x) = x(x)$ but by definition both functions are just the identity. Now if we wanted to see how an object is transformed *at a fixed point*, then we should compare $(\phi_* f)(x'(p))$ with $f(x(p))$, but this still would not correspond to the passive case. To make it correspond we need to express the transformed function in terms of the *old* coordinates (obviously this is only possible if $M = N$). To avoid confusion, call this new function $\tilde{f}$.

$$\begin{aligned} \tilde{f} : \mathbb{R}^n &\rightarrow \mathbb{R} \\ x(\phi p) &\mapsto \phi_*[f(x(p))] \equiv (\phi_* f)(x(\phi p)) = f((\phi_* x)(\phi p)) = f(x(p)) \\ x &\mapsto (\phi_* f)(x) = f(\phi_* x) \end{aligned} \tag{A.12}$$

We want to find transformation rules equivalent to (A.4) and (A.8) so introduce a vector field ξ and construct a diffeomorphism ϕ_t defined by moving each point an infinitesimal distance t along the integral curves of ξ. To first order in t, $x(\phi_t p) \approx x(p) + t\xi(p)$ and the transformed

function becomes

$$\begin{aligned}
\tilde{f}\left(x\left(p\right)\right) &= f\left(\left(\phi_{t*}x\right)\left(p\right)\right) \qquad (A.13)\\
&= f\left(x\left(\phi_t^{-1}p\right)\right)\\
&= f\left(x\left(\phi_{-t}p\right)\right)\\
&\approx f\left(x\left(p\right)\right) + t\left[\frac{\partial f\left(x\right)}{\partial x^\mu}\frac{\partial}{\partial t}\left[x^\mu\left(\phi_{-t}p\right)\right]\right]_{t=0}\\
&= f\left(x\left(p\right)\right) - t\partial_\mu f\left(x\left(p\right)\right)\xi^\mu\left(x\left(p\right)\right)\\
\tilde{f}\left(x\right) &\approx f\left(x\right) - \mathcal{L}_{t\xi}f\left(x\right) \qquad (A.14)
\end{aligned}$$

A vector field X acts on a function as a directional derivative $Xf \equiv \langle df, X\rangle = X^\mu\partial_\mu f$, giving another function. If g is a function on N, then from (A.9) we must have

$$X\left(p\right)\ \left(\phi^* g\right)\left(p\right) = \phi_*\left[X\left(p\right)\ \left(\phi^* g\right)\left(p\right)\right] = \left(\phi_* X\right)\left(\phi p\right)\ g\left(\phi p\right) \qquad (A.15)$$

so $\phi_*\left[X\left(p\right)\right] = \left(\phi_* X\right)\left(\phi p\right) = X\left(p\right)\phi^*$. Again, if we define $\phi_* X$ in terms of the new coordinates, we find that nothing changes:

$$\begin{aligned}
\left(\phi_* X\right)^\mu \frac{\partial}{\partial\left(\phi_* x\right)^\mu} g\left(\left(\phi_* x\right)\left(\phi p\right)\right) &= X^\alpha\left(x\left(p\right)\right)\partial_\alpha\phi^*\left[g\left(\left(\phi_* x\right)\left(\phi p\right)\right)\right] \qquad (A.16)\\
&= X^\alpha\partial_\alpha g\left(x\left(p\right)\right)\\
&= X^\alpha\frac{\partial x^\mu\left(p\right)}{\partial x^\alpha\left(p\right)}\frac{\partial}{\partial\left(\phi_* x\right)^\mu} g\left(\left(\phi_* x\right)\left(\phi p\right)\right)\\
&= X^\alpha\delta^\mu_\alpha\partial'_\mu g\left(\left(\phi_* x\right)\left(\phi p\right)\right)\\
\left(\phi_* X\right)^\mu\left(x\right) &= X^\mu\left(x\right) \qquad (A.17)
\end{aligned}$$

Though we are comparing components at two different points. In terms of the old coordinates on the other hand,

$$\begin{aligned}
\tilde{X}^\mu\left(x\left(\phi p\right)\right)\frac{\partial}{\partial x^\mu\left(\phi p\right)} g\left(x\left(\phi p\right)\right) &= X^\alpha\left(x\left(p\right)\right)\partial_\alpha\phi^*\left[g\left(x\left(\phi p\right)\right)\right] \qquad (A.18)\\
&= X^\alpha\left(x\left(p\right)\right)\partial_\alpha g\left(x\left(\phi p\right)\right)\\
&= X^\alpha\left(x\left(p\right)\right)J^\mu{}_\alpha\frac{\partial}{\partial x^\mu\left(\phi p\right)} g\left(x\left(\phi p\right)\right)
\end{aligned}$$

where $J^{\mu}_{\ \nu} \equiv \frac{\partial x^{\mu}(\phi_t p)}{\partial x^{\nu}(p)} = \delta^{\mu}_{\ \nu} + t\xi^{\mu}_{\ ,\nu}$. To first order in t, we get

$$\begin{aligned} \tilde{X}^{\mu}(x(p)) &\approx X^{\mu}\left(x\left(\phi_t^{-1}p\right)\right) + t\xi^{\mu}_{\ ,\alpha}X^{\alpha}\left(x\left(\phi_t^{-1}p\right)\right) \qquad \text{(A.19)} \\ &\approx X^{\mu}(x(p)) + t\,\frac{\partial X^{\mu}(x)}{\partial x^{\nu}}\frac{\partial x^{\nu}\left(\phi_{-t}p\right)}{\partial t}\bigg|_{t=0} + t\xi^{\mu}_{\ ,\alpha}X^{\alpha}(x(p)) \\ &= \left[X^{\mu} - t\partial X^{\mu}_{\ ,\nu}\xi^{\nu} + t\xi^{\mu}_{\ ,\nu}X^{\nu}\right](x(p)) \\ \tilde{X}^{\mu}(x) &\approx X^{\mu}(x) - \mathcal{L}_{t\xi}X^{\mu}(x) \qquad \text{(A.20)} \end{aligned}$$

This carries on to general tensors: thinking of them as maps from vectors and covectors to functions we find $(\phi_* T) = T\phi^*$ where the pull-back is applied to the vectors and covectors. As a function of the new coordinates the components don't change

$$(\phi_* T)^{\mu\cdots}_{\ \ \nu\cdots}(x) = T^{\mu\cdots}_{\ \ \nu\cdots}(x) \qquad \text{(A.21)}$$

but in terms of the old coordinates, they pick up a Lie derivative.

B. Calculation of the wave shape

The calculation of the gravitational wave shape can be done explicitly by starting with equation (3.23) and without going to Fourier space.

$$\begin{aligned}
\bar{h}^{\mu\nu}(x) &= 4G\int d^3y\,\frac{T^{\mu\nu}\left(t-|\boldsymbol{y}-\boldsymbol{x}|,\boldsymbol{y}\right)}{|\boldsymbol{y}-\boldsymbol{x}|} \qquad \text{(B.1)}\\
&= \frac{4G}{r}\int d^3y\,T^{\mu\nu}\left(t-r+\frac{\boldsymbol{x}}{r}\cdot\boldsymbol{y},\boldsymbol{y}\right)\\
&= \frac{4G\mu}{r}\int d^3y\int d^2\sigma\,\delta^{(3)}\left(\boldsymbol{y}-\mathbf{X}\right)\delta\left(t-r+\frac{\boldsymbol{x}}{r}\cdot\boldsymbol{y}-X^0\right)\left(\dot{X}^\mu\dot{X}^\nu-X'^\mu X'^\nu\right)\\
&= \frac{4G\mu}{r}\int d^2\sigma\,\delta\left(\hat{k}_x\cdot(X-x)\right)\left(\dot{X}^\mu\dot{X}^\nu-X'^\mu X'^\nu\right)
\end{aligned}$$

Where $\hat{k}_x=(1,\frac{\boldsymbol{x}}{r})$ is again the direction of the observer. We next go to null worldsheet coordinates.

$$\bar{h}^{\mu\nu}(x)=\frac{2G\mu}{r}\int d\sigma_+d\sigma_-\,\delta\left(t-r+\hat{k}_x\cdot\frac{1}{2}\left(X_++X_-\right)\right)\dot{X}_+^{(\mu}\dot{X}_-^{\nu)} \qquad \text{(B.2)}$$

$$\delta\left(t-r+\hat{k}_x\cdot\frac{1}{2}\left(X_++X_-\right)\right)=\frac{\delta\left(\sigma_+-\Sigma_+\right)}{\hat{k}_x\cdot\frac{1}{2}\dot{X}_+\left(\Sigma_+\right)} \qquad \text{(B.3)}$$

The value Σ_+ in the delta function will be complicated in general, but in the gravitational wave burst direction, $\hat{k}_x=\dot{X}_0$ and we have

$$\begin{aligned}
&\bar{h}^{\mu\nu}\left(t,r\dot{\mathbf{X}}_0\right) \qquad \text{(B.4)}\\
&= \frac{G\mu}{r}e_\oplus^{\mu\nu}\left|\ddot{X}_{+0}\right|\left|\ddot{X}_{-0}\right|\int d\sigma_+d\sigma_-\,\sigma_+\sigma_-\delta\left(t_R-\frac{1}{12}\left(\ddot{X}_{+0}^2\sigma_+^3+\ddot{X}_{-0}^2\sigma_-^3\right)\right)
\end{aligned}$$

The delta function will be zero unless

$$|t_R|<\frac{1}{12}\frac{l^3}{8}\left(\ddot{X}_{+0}^2+\ddot{X}_{-0}^2\right) \qquad \text{(B.5)}$$

This is the range in which the effects of our worldsheet are felt. Now let $\ddot{X}_<$ and $\ddot{X}_>$ be the smallest and largest respectively of $\left|\ddot{X}_{+0}\right|$ and $\left|\ddot{X}_{-0}\right|$. We do the $\sigma_>$ integral first assuming the delta function is not zero.

$$\delta\left(t_R - \frac{1}{12}\left(\ddot{X}_>^2\sigma_>^3 + \ddot{X}_<^2\sigma_<^3\right)\right) = \frac{\delta\left(\sigma_> - \left(\frac{12}{\ddot{X}_>^2}t_R - \frac{\ddot{X}_<^2}{\ddot{X}_>^2}\sigma_<^3\right)^{\frac{1}{3}}\right)}{\frac{3}{12}\ddot{X}_>^2\left(\frac{12}{\ddot{X}_>^2}t_R - \frac{\ddot{X}_<^2}{\ddot{X}_>^2}\sigma_<^3\right)^{\frac{1}{3}2}} \tag{B.6}$$

$$\begin{aligned}\bar{h}^{\mu\nu}\left(t, r\dot{\mathbf{X}}_0\right) &= \frac{4G\mu}{r}e_\oplus^{\mu\nu}\frac{\ddot{X}_<}{\ddot{X}_>}\int_{-\frac{l}{2}}^{\frac{l}{2}} d\sigma_<\,\sigma_<\left(\frac{12}{\ddot{X}_>^2}t_R - \frac{\ddot{X}_<^2}{\ddot{X}_>^2}\sigma_<^3\right)^{-\frac{1}{3}} \\ &= \frac{2G\mu l}{3r}e_\oplus^{\mu\nu}\left(\frac{\ddot{X}_<}{\ddot{X}_>}\right)^{\frac{1}{3}}T^{-\frac{1}{3}}\int_{-1}^{1} ds\, s^{-\frac{1}{3}}\left(1 - \frac{s}{T}\right)^{-\frac{1}{3}}\end{aligned} \tag{B.7}$$

We have introduced the normalized variables

$$s = \frac{8}{l^3}\sigma_<^3\ , \quad T = \frac{8}{l^3}\frac{12}{\ddot{X}_<^2}\left|t_R\right| \in \left[0, \frac{\ddot{X}_>^2 + \ddot{X}_<^2}{\ddot{X}_<^2}\right] \tag{B.8}$$

We must now ensure the limits of the $\sigma_>$ integral are respected. The requirement is $\frac{\ddot{X}_<^2}{\ddot{X}_>^2}\left|T - s\right| < 1$. Combining this with $|s| < 1$, the range of integration is now

$$\max\left(-1, T - \frac{\ddot{X}_>^2}{\ddot{X}_<^2}\right) < s < 1 \tag{B.9}$$

The lower bound will change when

$$\begin{aligned}\frac{\ddot{X}_>^2}{\ddot{X}_<^2} - T &= 1 \\ \left|t_R\right| &= \frac{1}{12}\frac{l^3}{8}\left(\ddot{X}_>^2 - \ddot{X}_<^2\right)\end{aligned} \tag{B.10}$$

Things get a bit complicated now and we must calculate the integral in 5 cases.

1. $T < \frac{\ddot{X}_>^2}{\ddot{X}_<^2} - 1$ and $T < 1$

$$\bar{h}^{\mu\nu}\left(t, r\dot{\mathbf{X}}_0\right) = \frac{G\mu l}{r} e_\oplus^{\mu\nu} \left(\frac{\ddot{X}_<}{\ddot{X}_>}\right)^{\frac{1}{3}} \left(\frac{2\sqrt{3}}{\pi} T^{\frac{1}{3}} \Gamma\left(\frac{2}{3}\right)^3 - \frac{4}{3}(1-T)^{\frac{2}{3}} - \frac{2}{3}(T+1)\ {}_2F_1\left[\frac{1}{3}, \frac{2}{3}; \frac{5}{3}; T\right] - T^{-\frac{1}{3}}\ {}_2F_1\left[\frac{1}{3}, \frac{2}{3}; \frac{5}{3}; -\frac{1}{T}\right]\right) \tag{B.11}$$

2. $1 < T < \frac{\ddot{X}_>^2}{\ddot{X}_<^2} - 1$. This happens if $\ddot{X}_>^2 > 2\ddot{X}_<^2$.

$$\begin{aligned} &\bar{h}^{\mu\nu}\left(t, r\dot{\mathbf{X}}_0\right) \\ &= \frac{G\mu l}{r} e_\oplus^{\mu\nu} \left(\frac{\ddot{X}_<}{\ddot{X}_>}\right)^{\frac{1}{3}} T^{-\frac{1}{3}} \left({}_2F_1\left[\frac{1}{3}, \frac{2}{3}; \frac{5}{3}, \frac{1}{T}\right] - {}_2F_1\left[\frac{1}{3}, \frac{2}{3}; \frac{5}{3}, -\frac{1}{T}\right]\right) \end{aligned} \tag{B.12}$$

3. $\frac{\ddot{X}_>^2}{\ddot{X}_<^2} - 1 < T < 1$. Here the lower bound increases with T, from -1 to $+1$. We define $V = \frac{\ddot{X}_>^2}{\ddot{X}_<^2} - T$.

$$\begin{aligned} &\bar{h}^{\mu\nu}\left(t, r\dot{\mathbf{X}}_0\right) \\ &= \frac{2G\mu l}{3r} e_\oplus^{\mu\nu} \left(\frac{\ddot{X}_<}{\ddot{X}_>}\right)^{\frac{1}{3}} T^{-\frac{1}{3}} \left(\int_0^1 ds\, s^{-\frac{1}{3}} \left(1 - \frac{s}{T}\right)^{-\frac{1}{3}} - \int_0^V ds\, s^{-\frac{1}{3}} \left(1 + \frac{s}{T}\right)^{-\frac{1}{3}}\right) \\ &= \frac{2G\mu l}{3r} e_\oplus^{\mu\nu} \left(\frac{\ddot{X}_<}{\ddot{X}_>}\right)^{\frac{1}{3}} T^{-\frac{1}{3}} \\ &\quad \times \left[\left(\int_0^T + \int_T^1\right) ds\, s^{-\frac{1}{3}} \left(1 - \frac{s}{T}\right)^{-\frac{1}{3}} - V^{\frac{2}{3}} \int_0^1 dq\, q^{-\frac{1}{3}} \left(1 + \frac{V}{T} q\right)^{-\frac{1}{3}}\right] \\ &= \frac{G\mu l}{r} e_\oplus^{\mu\nu} \left(\frac{\ddot{X}_<}{\ddot{X}_>}\right)^{\frac{1}{3}} \left[\frac{2\sqrt{3}}{\pi} T^{\frac{1}{3}} \Gamma\left(\frac{2}{3}\right)^3 - \frac{4}{3}(1-T)^{\frac{2}{3}} \right. \\ &\quad \left. - \frac{2}{3}(T+1)\ {}_2F_1\left[\frac{1}{3}, \frac{2}{3}; \frac{5}{3}; T\right] - T^{-\frac{1}{3}} V^{\frac{2}{3}}\ {}_2F_1\left[\frac{1}{3}, \frac{2}{3}; \frac{5}{3}, -\frac{V}{T}\right]\right] \end{aligned} \tag{B.13}$$

4. $1 < T$ and $\frac{\ddot{X}_>^2}{\ddot{X}_<^2} - 1 < T < \frac{\ddot{X}_>^2}{\ddot{X}_<^2}$

$$\begin{aligned}\bar{h}^{\mu\nu}\left(t, r\dot{\mathbf{X}}_0\right) &= \frac{G\mu l}{r} e_\oplus^{\mu\nu} \left(\frac{\ddot{X}_<}{\ddot{X}_>}\right)^{\frac{1}{3}} \left({}_2F_1\left[\frac{1}{3}, \frac{2}{3}; \frac{5}{3}, \frac{1}{T}\right] - \frac{4}{3}(1-T)^{\frac{2}{3}}\right. \\ &\left. -\frac{2}{3}(T+1)\ {}_2F_1\left[\frac{1}{3}, \frac{2}{3}; \frac{5}{3}; T\right] - T^{-\frac{1}{3}} V^{\frac{2}{3}}\ {}_2F_1\left[\frac{1}{3}, \frac{2}{3}; \frac{5}{3}, -\frac{V}{T}\right]\right)\end{aligned} \tag{B.14}$$

5. $\frac{\ddot{X}_>^2}{\ddot{X}_<^2} < T < \frac{\ddot{X}_>^2}{\ddot{X}_<^2} + 1$

$$\bar{h}^{\mu\nu}\left(t, r\dot{\mathbf{X}}_0\right) = \frac{G\mu l}{r} e_\oplus^{\mu\nu} \left(\frac{\ddot{X}_<}{\ddot{X}_>}\right)^{\frac{1}{3}} T^{-\frac{1}{3}} \left({}_2F_1\left[\frac{1}{3}, \frac{2}{3}; \frac{5}{3}, \frac{1}{T}\right] - V^{\frac{2}{3}}\ {}_2F_1\left[\frac{1}{3}, \frac{2}{3}; \frac{5}{3}, -\frac{V}{T}\right]\right) \tag{B.15}$$

The simplest case is when $\left|\ddot{X}_+\right| = \left|\ddot{X}_-\right|$. Then we only need two pieces (3 and 5) for $T \in [0,1]$ and $[1,2]$. This is the first wave shown in figure 4.3 ($a = 1$). We can also get the value at $t_R = 0$:

$$\bar{h}^{\mu\nu}\left(r\dot{X}_0\right) = -\frac{4G\mu l}{r} e_\oplus^{\mu\nu} \left(\frac{\ddot{X}_<}{\ddot{X}_>}\right)^{\frac{1}{3}} \tag{B.16}$$